Corrosion Engineering Approach to Rapidly Preparing Ni(Fe)OOH/Ni(Fe)S$_x$ Nanosheet Array for Efficient Water Oxidation

Mingyue Chen, Wenhui Li, Yu Lu, Pengcheng Qi, Hao Wu, Gaofu Liu, Yue Zhao, and Yiwen Tang*

Institute of Nano-Science & Technology, College of Physical Science and Technology, Central China Normal University,

Wuhan 430079, China

*Corresponding author: Tel.: +86-27-67867947; Fax: +86-27-67861185;

E-mail: ywtang@ccnu.edu.cn

Experimental Section

Materials and chemicals: Ni foam (NF), Fe foam (FF), and NiFe alloy foam (NFF), Nickel chloride hexahydrate (NiCl$_2$·6H$_2$O, Sinopharm Chemical ReagentCo., Ltd, shanghai), Ferric trichloride hexahydrate (FeCl$_3$·6H$_2$O, Sinopharm Chemical ReagentCo., Ltd, shanghai), ammonium persulfate ((NH$_4$)$_2$S$_2$O$_8$, Sinopharm Chemical ReagentCo., Ltd, shanghai), thiourea ((NH$_2$)$_2$CS, Sinopharm Chemical ReagentCo., Ltd, shanghai) were used. All reagents were of analytical pure grade and were not further processed.

Syntiesis of Ni(Fe)OOH/Ni(Fe)S$_x$ nanosheet arrays. Solution was formed by mixing (NH$_4$)$_2$S$_2$O$_8$ (3 mmol), (NH$_2$)$_2$CS (4 mmol), and FeCl$_3$ (1 mmol) in 10 mL of deionized (DI) water. NiFe foam with dimension of 1*4 cm^2 was immersed in the mixed solution. After 10 minutes, the NiFe foam was taken out, washed with DI water and absolute ethanol three times, and then dried with a blower. The prepared sample was marked as Ni(Fe)OOH/Ni(Fe)S$_x$. When the molar amount of (NH$_4$)$_2$S$_2$O$_8$ in the mixed solution became 4 mmol, 2 mmol, and 1mmol, under the same synthesis conditions, the prepared samples were marked as Ni(Fe)OOH/Ni(Fe)S$_x$-4, Ni(Fe)OOH/Ni(Fe)S$_x$-2, and Ni(Fe)OOH/Ni(Fe)S$_x$-1, respectively. When solution was formed by mixing (NH$_4$)$_2$S$_2$O$_8$ (3 mmol), (NH$_2$)$_2$CS (4 mmol), NiCl$_2$•6H$_2$O (1 mmol) in 10 mL of DI water, the sample prepared after 10 minutes of etching is marked as Ni(Fe)OOH/Ni(Fe)S$_x$-Ni. When solution was formed by mixing (NH$_4$)$_2$S$_2$O$_8$ (3 mmol) and (NH$_2$)$_2$CS (4 mmol) in 10 mL of DI water, the sample prepared after 10 minutes of etching is marked as Ni(Fe)OOH/Ni(Fe)S$_x$-

H$_2$O.

Synthesis of NiOOH/NiS$_x$ and FeOOH/FeS$_x$. (NH$_4$)$_2$S$_2$O$_8$ (3 mmol), (NH$_2$)$_2$CS (4 mmol), and FeCl$_3$ (1 mmol) were dissolved in 10 mL of DI water to form a corrosion solution. Then the Fe foam with an area of 1*4 cm^2 was immersed in the corrosion solution, after 10 minutes, the etched Fe foam was taken out and washed with DI water and absolute ethanol three times, and then dired with a blower, the sample was marked as FeOOH/FeS$_x$. (NH$_4$)$_2$S$_2$O$_8$ (3 mmol) and (NH$_2$)$_2$CS (4 mmol) were dissolved in 10 mL of DI water to form a corrosion solution. Then the Ni foam with an area of 1*4 cm^2 was immersed in the corrosion solution, after 10 minutes, the etched Ni foam was taken out and washed with DI water and absolute ethanol three times, and then dired with a blower, the sample was marked as NiOOH/NiSx.

Synthesis of Ni(Fe)OOH. (NH$_4$)$_2$S$_2$O$_8$ (3 mmol) and NaOH (9 mmol) were dissolved in 10 mL of DI water to form a corrosion solution, then the NiFe foam with an area of 1*4 cm^2 was immersd in the corrosion solution, after 24 h, the etched NiFe foam was taken out and washed with DI water and absolute ethanol three times, and dired with a blower, the sample was marked as Ni(Fe)OOH.

Synthesis of Mo$_2$C/MoO$_2$/MoNi$_4$. NiMoO$_4$ arrays were constructed on nickel foam through a hydrothermal reaction. In brief, 2 mmol Ni(NO$_3$)$_2$•6H$_2$O and 0.5 mmol (NH$_4$)$_6$Mo$_7$O$_{24}$•4H$_2$O were dissolved in 50 ml of DI water in a Teflon liner at room temperature, then the treated Ni foam substrate (2*5 cm^2) was immersed in this solution and heated 150 °C for 6 h, after cooling down room temperature, the NiMoO$_4$/NF was taken out and washed with DI water and ethanol, followed by drying with a bolwer. Finally, Mo$_2$C/MoO$_2$/MoNi$_4$ was obtained through a one-step annealing process. Specifically, a quartz crucible containing 1 ml ethanol was placed on the upper end of the tube furnace, wherein ethanol was used as a reducing agent and a carbon source, and NiMoO$_4$ arrays were placed in the middle of the tube furnace and heated at 600 °C for 2 h in a N$_2$ atmosphere, and then, the Mo$_2$C/MoO$_2$/MoNi$_4$ electrocatalyst was obtained.

Characterizations. The morphologies and elemental analysis of the samples were examined by scanning electron microscopy (SEM, JSM-7900, JEOL) equipped with an energy dispersive X-ray spectroscopy (EDS, Oxford). The surface chemical composition and valence states of the elements were measured by X-ray photoelectron spectroscopy (XPS,

Thermo VG Multilab 2000) with X-ray radiation of 1486.6 eV and assigning the C 1s peak to 284.6 eV. The crystalline phases and elemental analysis of the samples were analyzed by Transmission electron microscopy (TEM, JEM-F200, JEOL) equipped with an ESD. Contact angle was measured on XG-CAMB3 (CA, Xuanzhun instrument, XG-CAMB3, China). Raman spectrum of the electrodes were collected on HORIBA LabRAM Spectrometer with the laser of 532 nm. Atomic force microscopy (AFM, Multimode Nanoscope IIIa, Veeco Instruments) was used to determine the thickness of the electrode materials.

Electrochemical measurements. OER performances of all samples were investigated in a three-electrode cell containing in 1 M KOH aqueous solution. The prepared samples were used as the working electrode, a graphite rod as the counter electrode, and Hg/HgO (contains 1M KOH solution) is used as the reference electrode. Linear sweep voltammetry (LSV), cyclic voltammetry (CV), and chronopotentiometry tests were performed to evaluate the OER activity and long-term stability of the samples on an electrochemical workstation (Chenhua instrument, CHI660E, Shanghai Chenhua Instrument Co. Ltd., China). Electrochemical impedance spectroscopy (EIS) measurements were conducted in a frequency range from 100 kHz to 0.01 Hz with an AC potential amplitude of 5 mV on an electrochemical workstation (CHI660E). Before the electrochemical test, the electrolyte was bubled with high-purity Ar for over 10 minutes to remove the dissolved oxygen in the KOH aqueous solution. All potentials in this work refer to Reversible Hydrogen Electrode (RHE) by converting the value ($E_{RHE} = E_{test} + E_{Hg/HgO} + 0.059 \times pH$) with iR-compensation, the R value was determined by the EIS test. In addition, the RHE potential was calibrated by the initial potential of the hydrogen evolution reaction (HER) of metal Pt in 1 M KOH aqueous solution. And the overpotential (η) of OER was calculated with the equation:

$$\eta_{OER} = E_{RHE} - 1.23$$

Overpotential of HER was calculated with the equation:

$$\eta_{HER} = 0 - E_{RHE}$$

The electrochemical active surface area (ECSA) were investigated using the double layer capacitances (C_{dl}). The specific capacitance for a 3D metal foam (Ni foam; Fe foam; and NiFe foam) surface is supposed to be about 60 μF cm^{-2}, and the ECSA is estimated by the following formule:

$$ECSA = C_{dl}(\mu F\ cm^{-2})/60\mu F\ cm^{-2}\ per\ cm^2\ ECSA$$

Calculation of faradaic efficiency: Faradaic efficiency (FE) for OER was determined using a drainage method at room temperature. Briefly, the Ni(Fe)OOH/Ni(Fe)S$_x$ worked at a constant current density of 50 mA cm^{-2} in 1 M KOH aqueous solution and the volume (V) of gas products was recorded every 20 min. FE was calculated based on the equation: FE = V / [Vm $\times$ I $\times$ t / (n $\times$ F)] $\times$ 100%, where V is the volume of the gas products (L), Vm is the standard molar volume (24.4 L molL^{-1}), I is the current (A), t is the time (s), n is the number of electrons involved in generating one molecule of a gas product (4 for oxygen gas), and F is the Faraday constant (96485.3 C molL^{-1}).

Calculation of TOF: the turnover frequency (TOF) value of OER was estimated using the following equation

TOF=[Number of total oxygen turn overs / geometrical area (cm^2)] / [Number of surface active sites / geometrical area (cm^2)]

The total number of oxygen turn overs:

Number of O$_2$= [j (mA cm^{-2})] $\times$ [(1 C s^{-1}) / 1000 mA] $\times$ [(6.02 $\times$ 10^{23} O$_2$ molecules) / (1 mol O$_2$)] $\times$ [(1 mol e$^-$) / 96485.3 C] $\times$ [(1 mol O$_2$) / (2 mol e$^-$)]

$$= 1.56 \times 10^{15}\ O_2\ s^{-1} / cm^2$$

The number of active sites as the total number of the surface sites was estimated from the roughness factor together with the unit cell of the catalysts, which will validly evaluate the actual TOF. The surface active sites per unit of actual surface area cab be calculated using the following equations:

Number of active sites = [(Nubmer of atoms per unit cell) / (Volume per unit cell)]$^{2/3}$

Number of actives sites (NiOOH) = [(12 atoms per unit cell) / (141.46 Å^3 per unit cell)] = 1.93 $\times$ 10^{15} atoms cm^{-2}

Number of active sites (FeOOH) = [(16 atoms per unit cell) / (138.62 Å^3 per unit cell)] = 2.37 $\times$ 10^{15} atoms cm^{-2}

Number of active sites (Ni$_9$S$_8$) = [(68 atoms per unit cell) / (977.8 Å^3 per unit cell)] = 1.69 $\times$ 10^{15} atoms cm^{-2}

Thus, the number of the active sites for NiFeOOH/NiFeSx is around 2.00 $\times$ 10^{15} atoms cm^{-2} and that for NiOOH/NiSx is around 1.81 $\times$ 10^{15} atoms cm^{-2}. In the FeOOH/FeS$_x$ electrode material, the surface FeS$_x$ is oxidized to sulfate with low content, therefore, the number of the active sites for FeOOH/FeS$_x$ is equated to the number of active sites of FeOOH, and the number

of active sites is 2.37 $\times$ 10^{15} atoms cm^{-2}. The number of the active sites for Ni(Fe)OOH is around 2.15 $\times$ 10^{15} atoms cm^{-2}.

The plots of current density can be converted into TOF plots using the following formula:

$$TOF_{OER} = [1.56 \times 10^{15} \, O_2 \, s^{-1}/cm_2 \times j] / (\text{Number of active sites} \times ECSA)$$
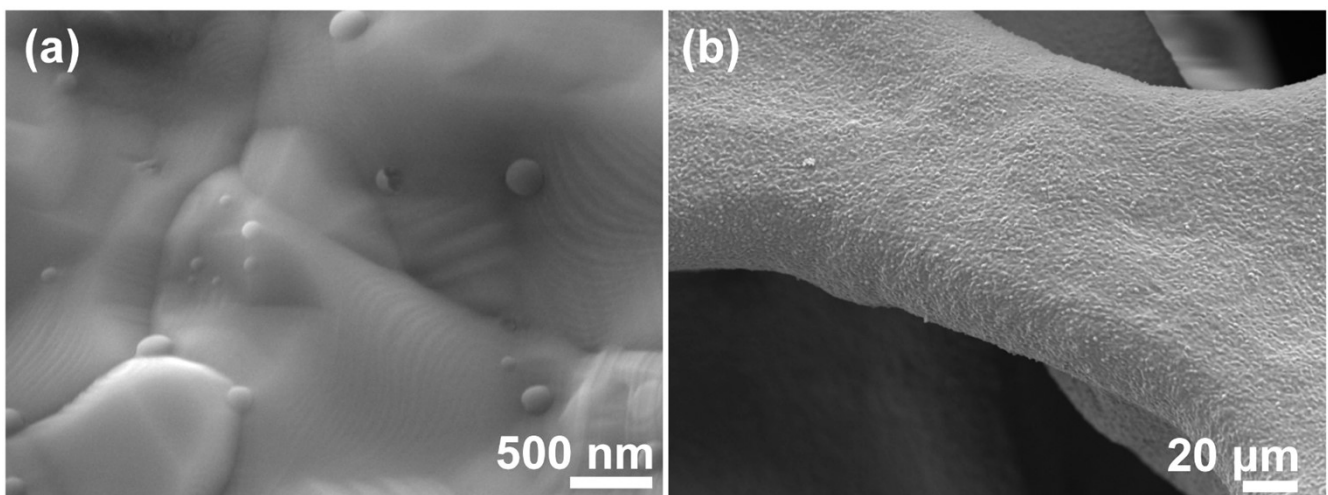
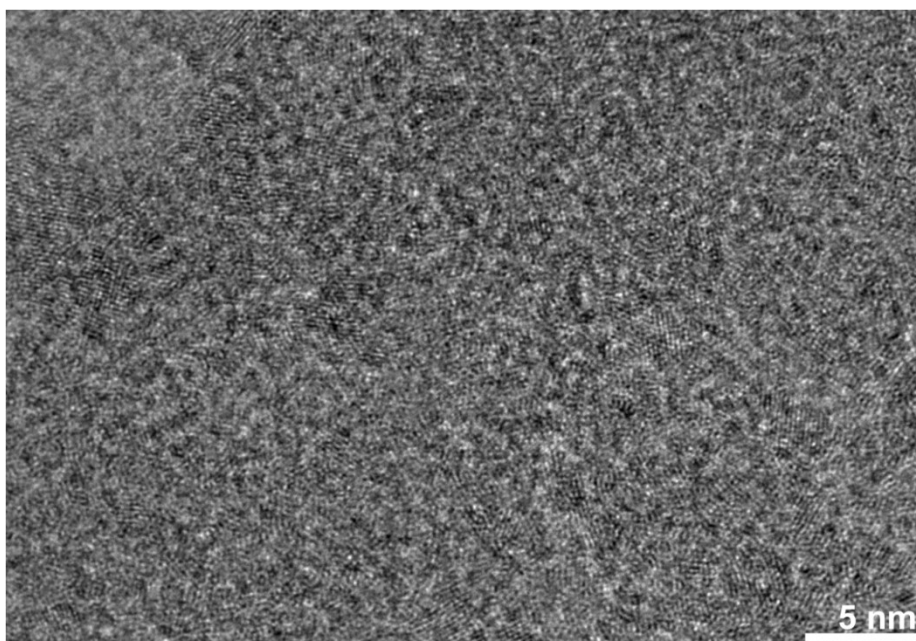**Figures and Tables**

Figure s1 SEM images of NiFe foam.

Figure s2 HRTEM image of the Ni-Fe composites nanosheets array on the surface of NiFe foam.
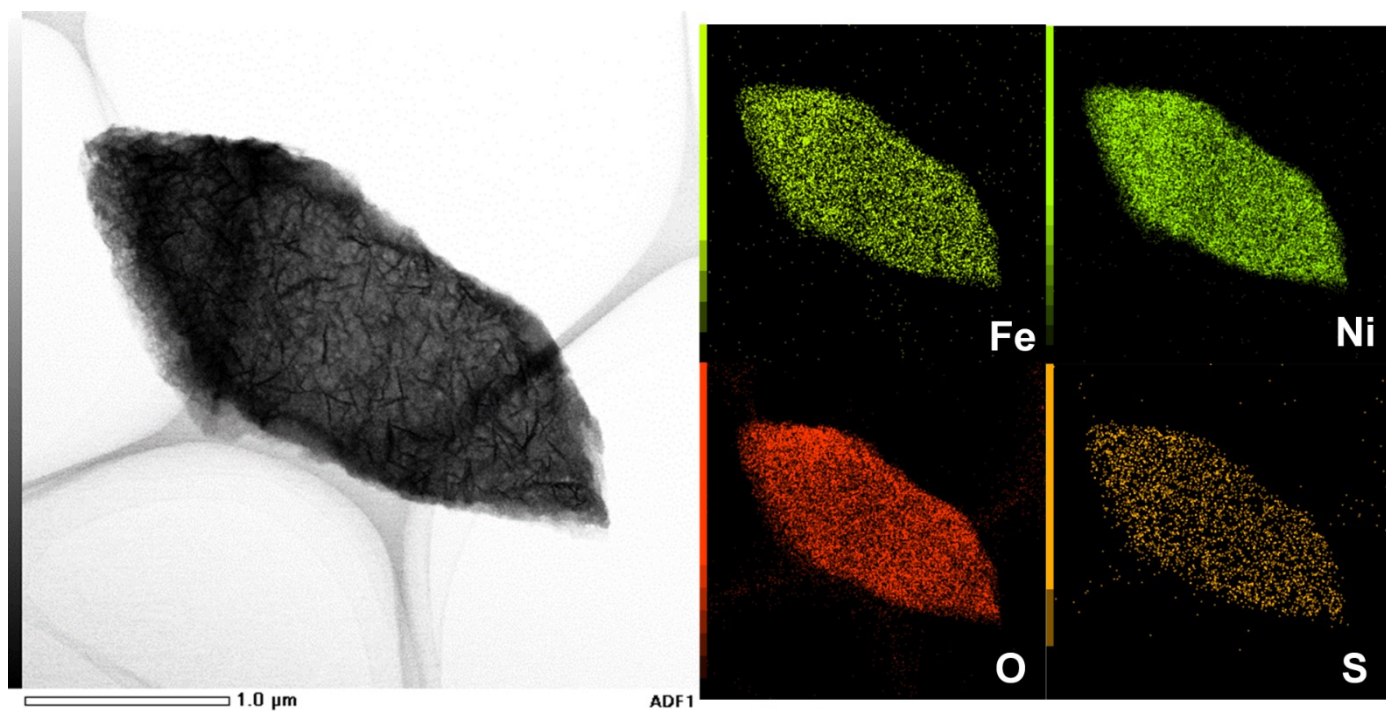
Figure s3 STEM image of the Ni-Fe composites nanosheets array and the corresponding elemental mapping images.
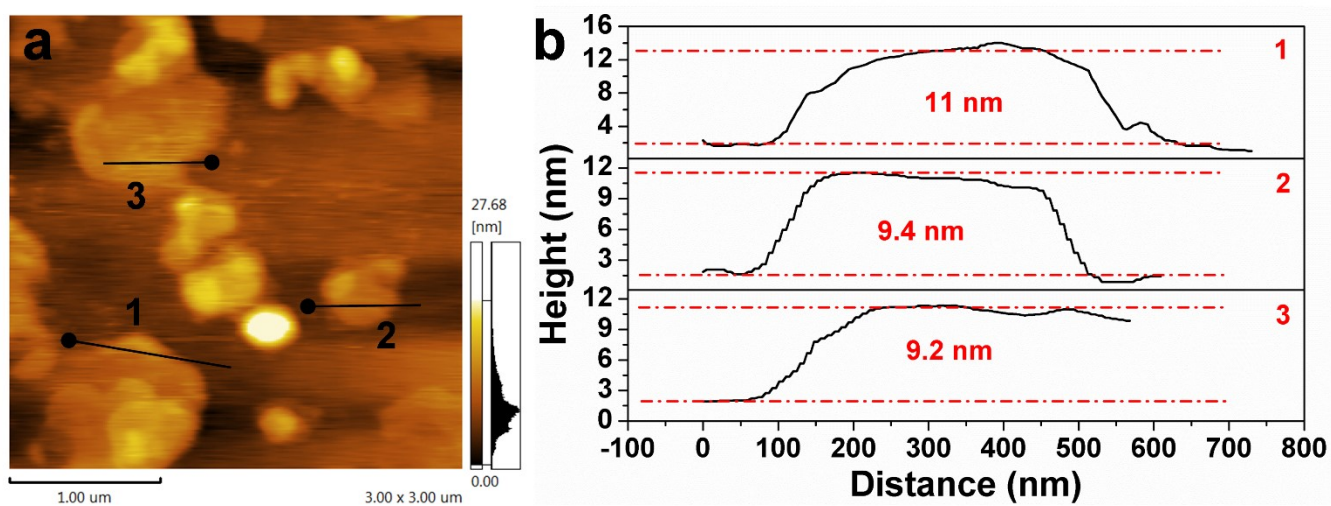
Figure s4 (a) AFM height profiles of Ni(Fe)OOH/Ni(Fe)S$_x$; the numbers 1–3 in (a) correspond to the profiles 1–3 in (b).
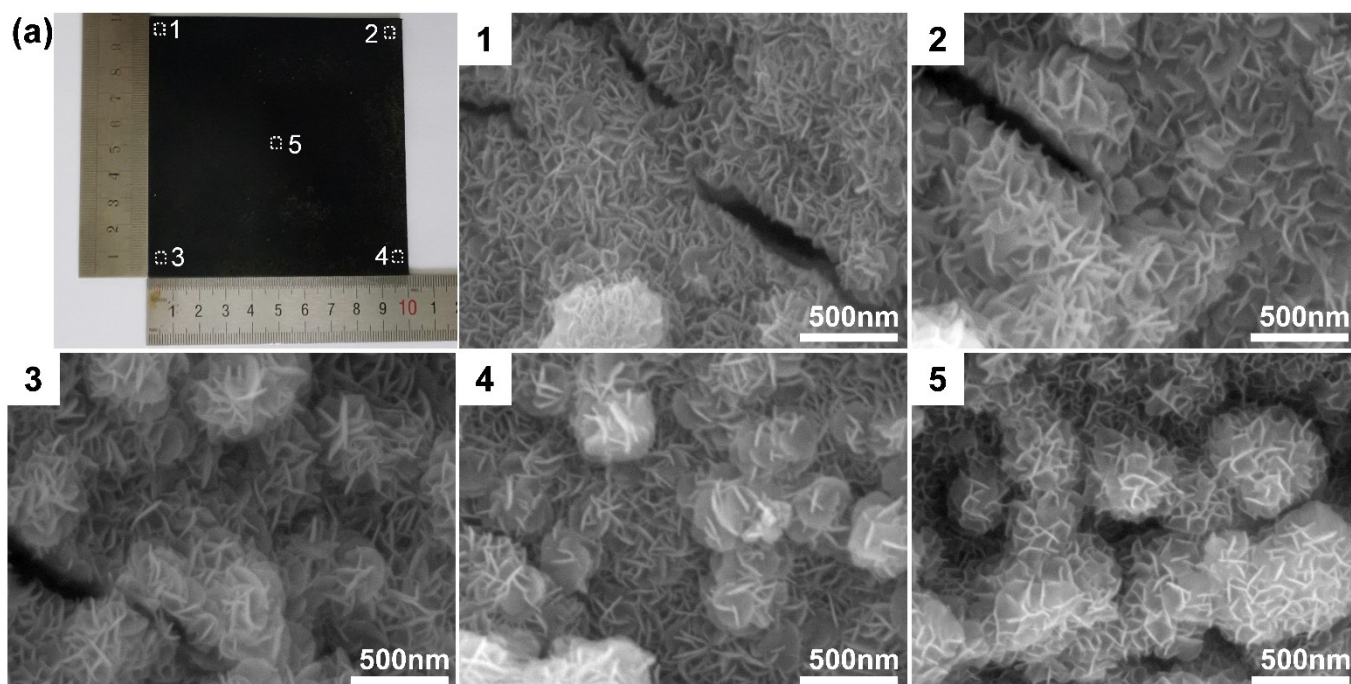
Figure s5 Digital image of a material (10X10 cm^2) obtained from a scaled-up corrosion engineering in the aqueous solution containing $(NH_4)_2S_2O_8$, $(NH_2)_2CS$, and $FeCl_3$ and the corresponding SEM images of the representative areas 1-5.
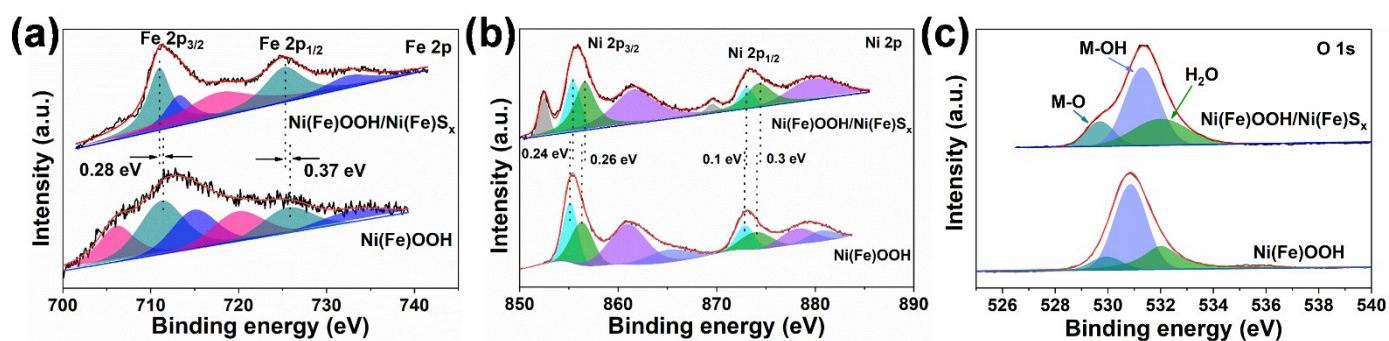
Figure s6 High-resolution (a) Fe 2p, (b) Ni 2p, and (c) O 1s of Ni(Fe)OOH/Ni(Fe)S$_x$ and Ni(Fe)OOH.
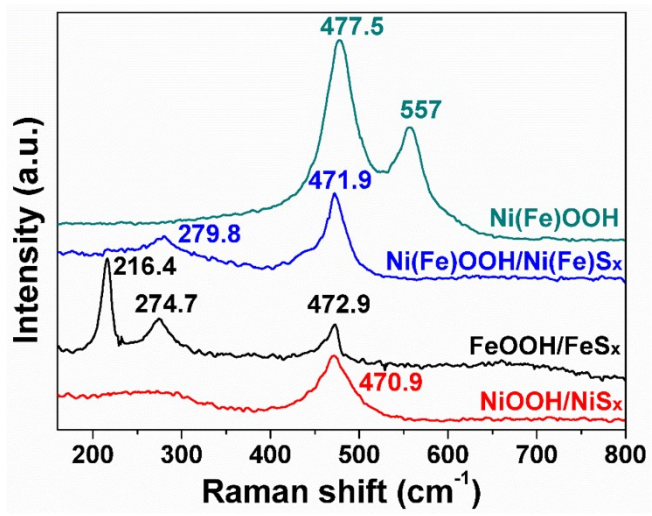
Figure s7 Raman spectra of various samples.
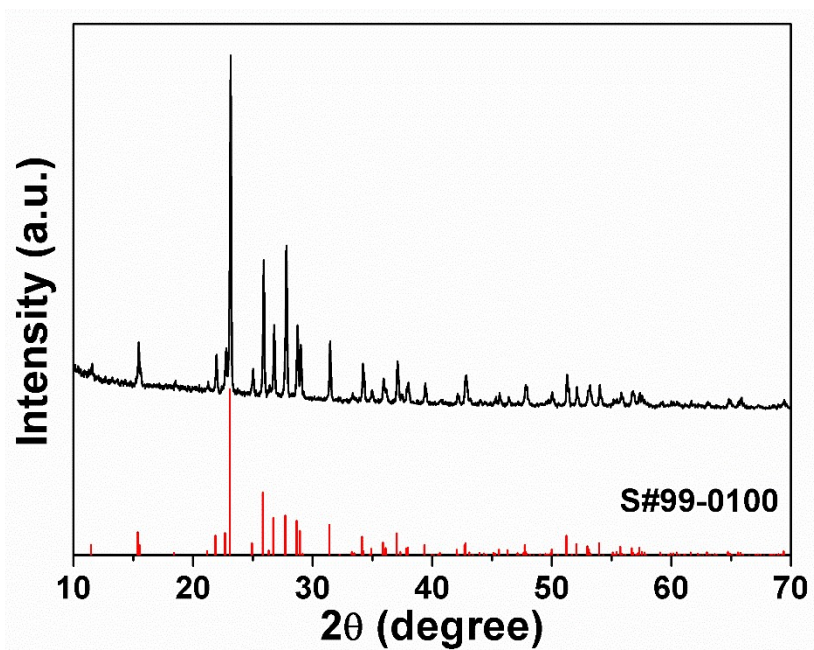
Figure s8 XRD patterns of the S .

電子图像 1 Fe Kα1 Ni Lα1,2 O Kα1
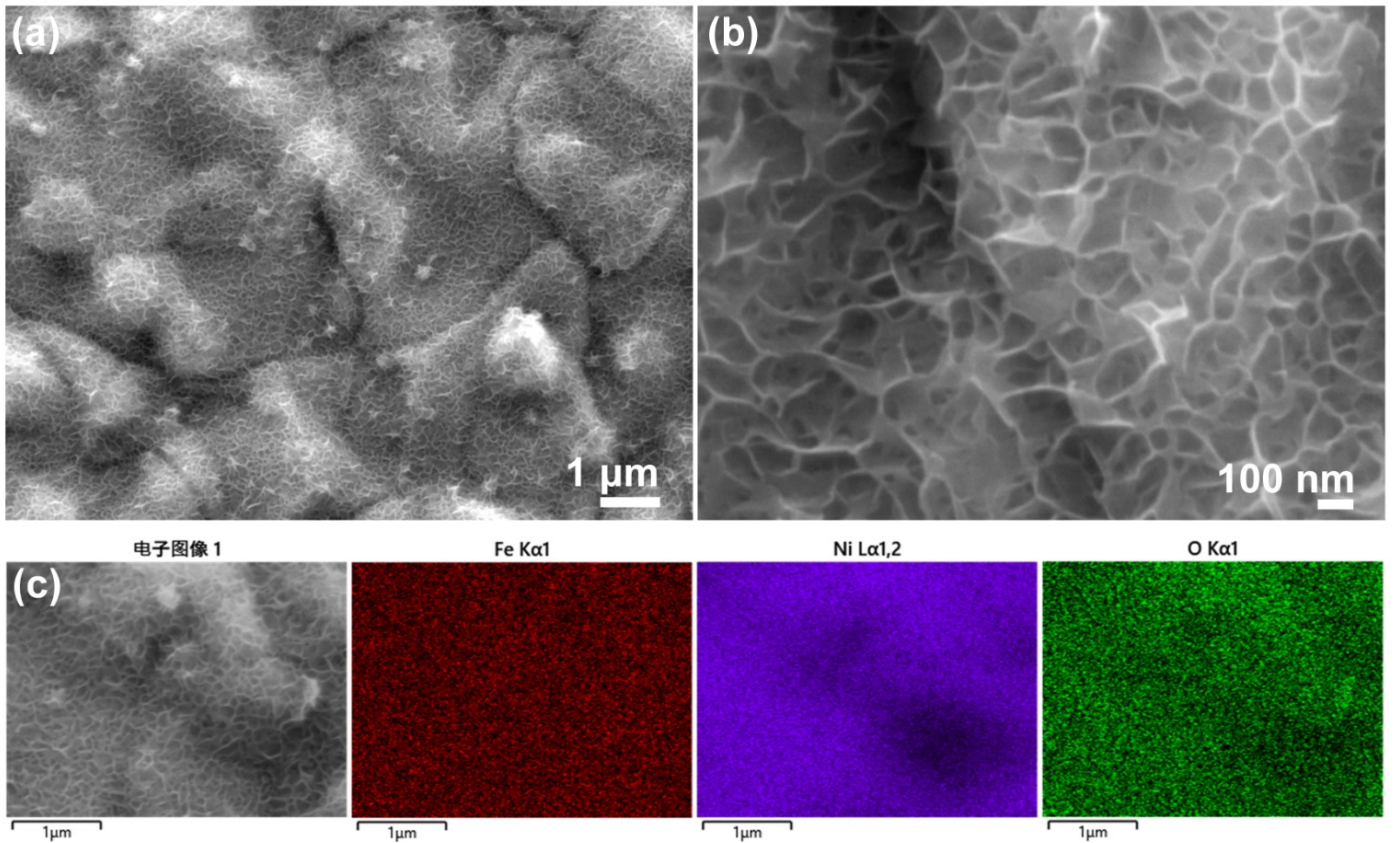
Figure s9 (a), (b) SEM images of the Ni(Fe)OOH and (c) corresponding elemental mapping images.
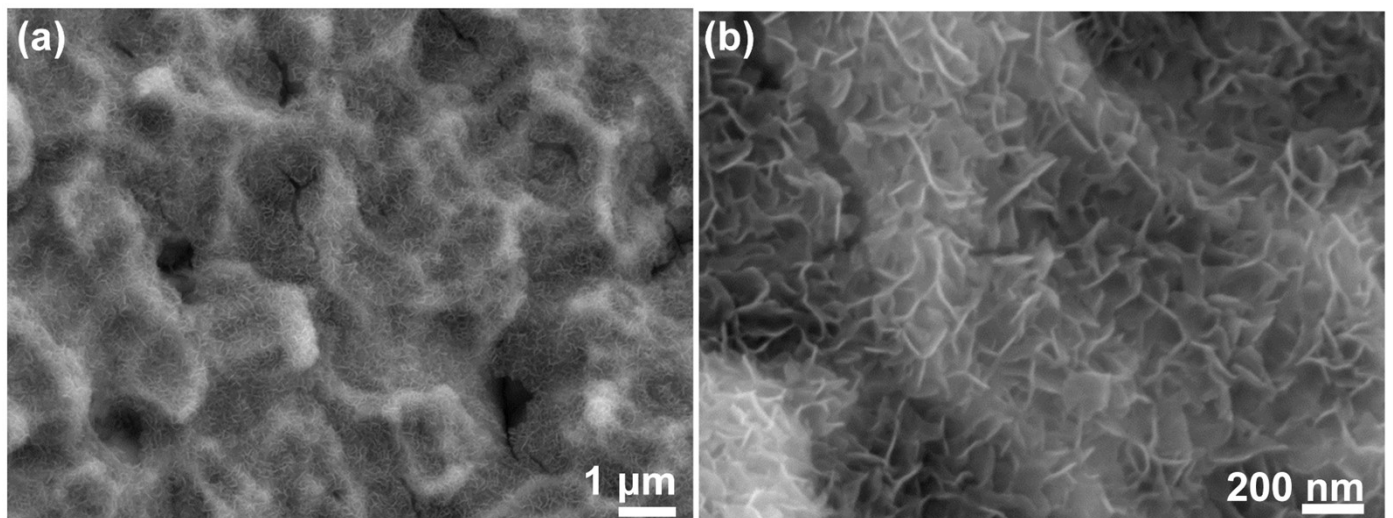
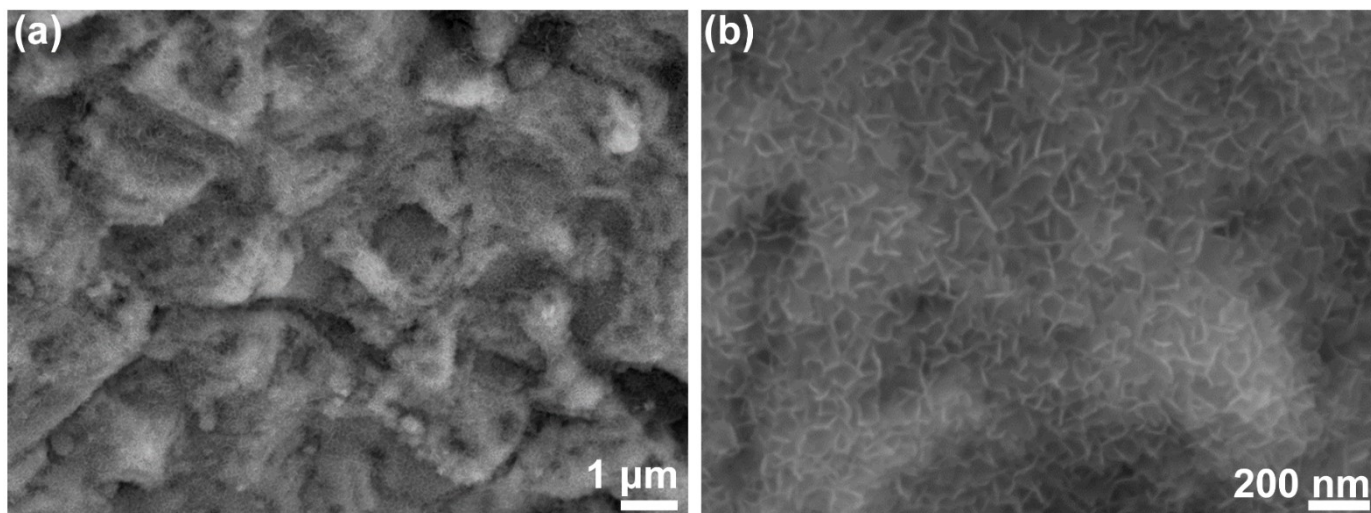Figure s10 (a), (b) SEM images of the Ni(Fe)OOH/Ni(Fe)S_x-Ni

11

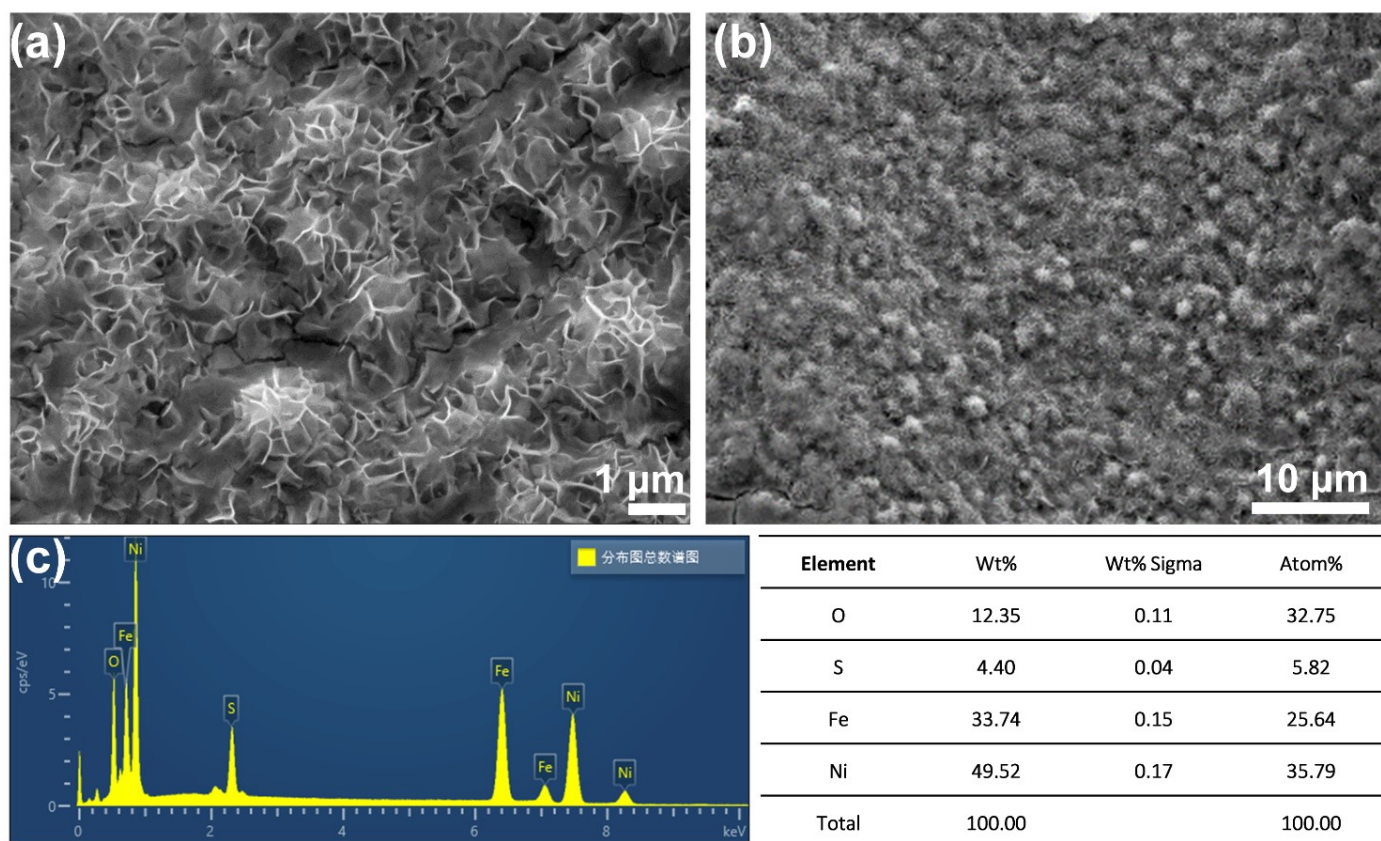Figure s11 (a), (b) SEM images of the Ni(Fe)OOH/Ni(Fe)S$_x$-H$_2$O.

Element	Wt%	Wt% Sigma	Atom%
O	12.35	0.11	32.75
S	4.40	0.04	5.82
Fe	33.74	0.15	25.64
Ni	49.52	0.17	35.79
Total	100.00		100.00

Figure s12 (a), (b) SEM images of the Ni(Fe)OOH/Ni(Fe)S$_x$-1; (c) EDS analysis of Ni(Fe)OOH/Ni(Fe)S$_x$-1 and corresponding element ratios.
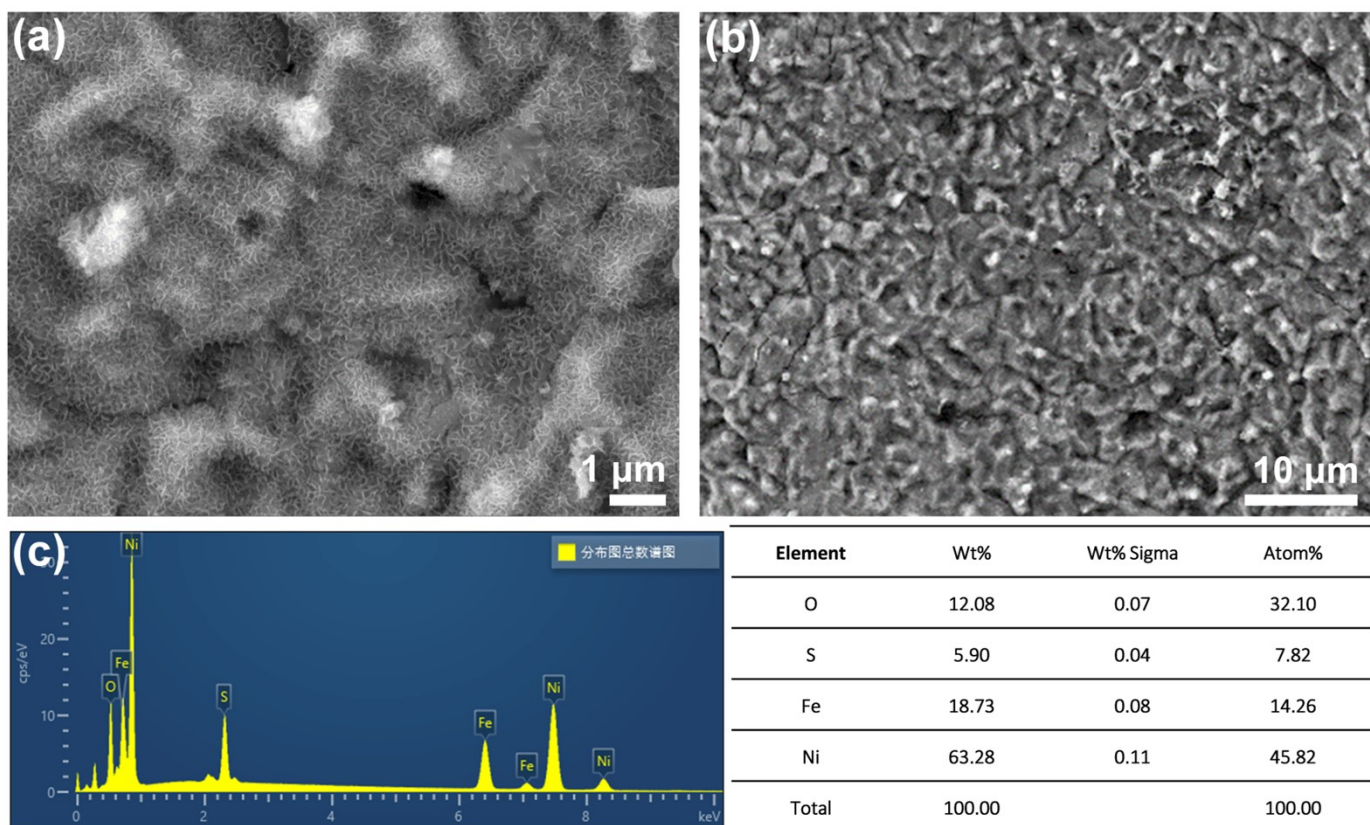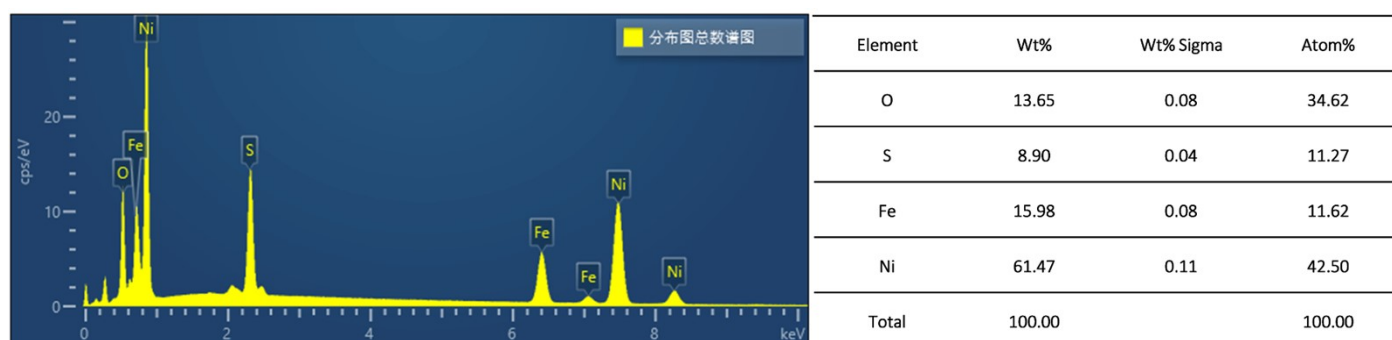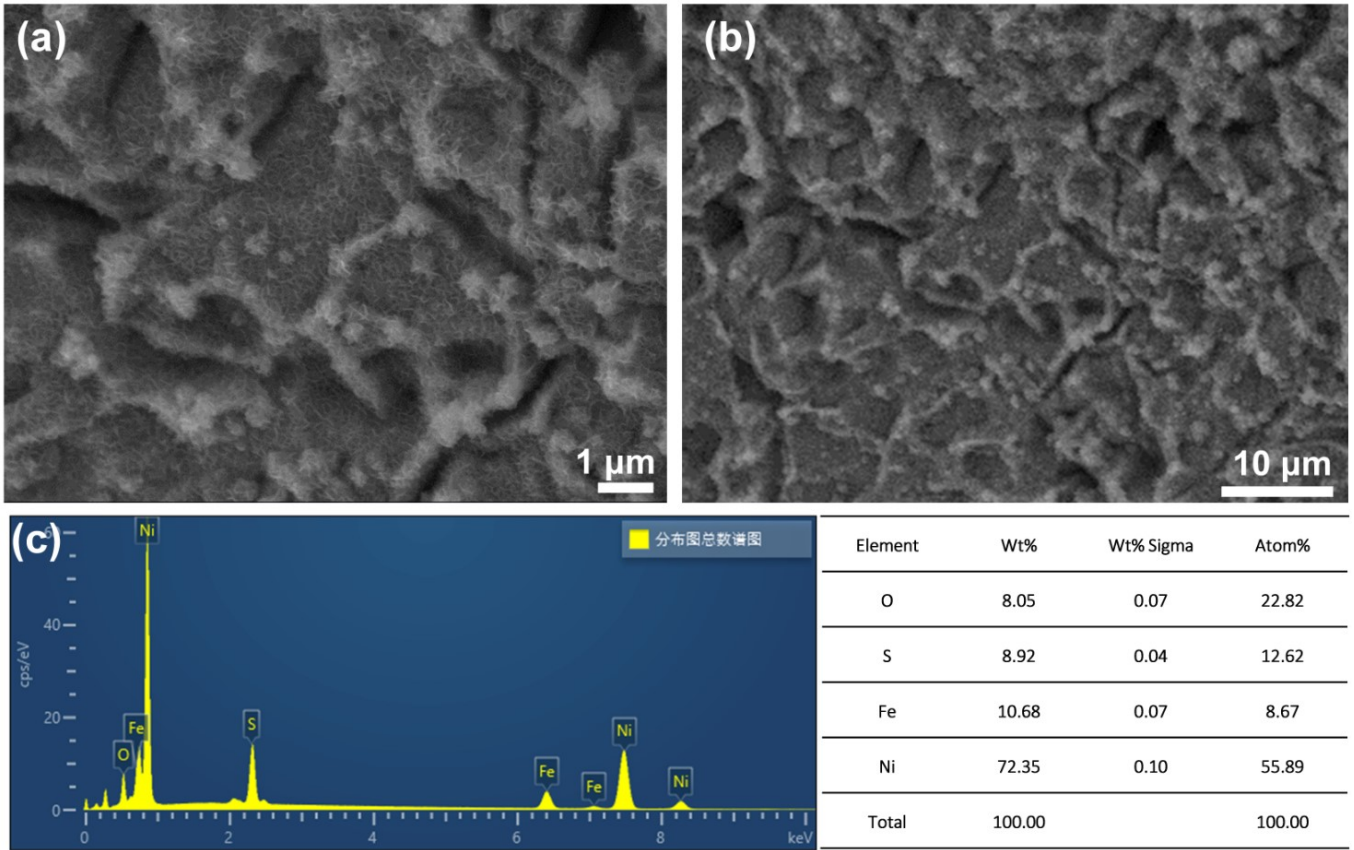
Element	Wt%	Wt% Sigma	Atom%
O	12.08	0.07	32.10
S	5.90	0.04	7.82
Fe	18.73	0.08	14.26
Ni	63.28	0.11	45.82
Total	100.00		100.00

Figure s13 (a), (b) SEM images of the Ni(Fe)OOH/Ni(Fe)S$_x$-2; (c) EDS analysis of Ni(Fe)OOH/Ni(Fe)S$_x$-2 and corresponding element ratios.

Element	Wt%	Wt% Sigma	Atom%
O	13.65	0.08	34.62
S	8.90	0.04	11.27
Fe	15.98	0.08	11.62
Ni	61.47	0.11	42.50
Total	100.00		100.00

Figure s14 EDS analysis of Ni(Fe)OOH/Ni(Fe)S$_x$ and corresponding element ratios.

Element	Wt%	Wt% Sigma	Atom%
O	8.05	0.07	22.82
S	8.92	0.04	12.62
Fe	10.68	0.07	8.67
Ni	72.35	0.10	55.89
Total	100.00		100.00

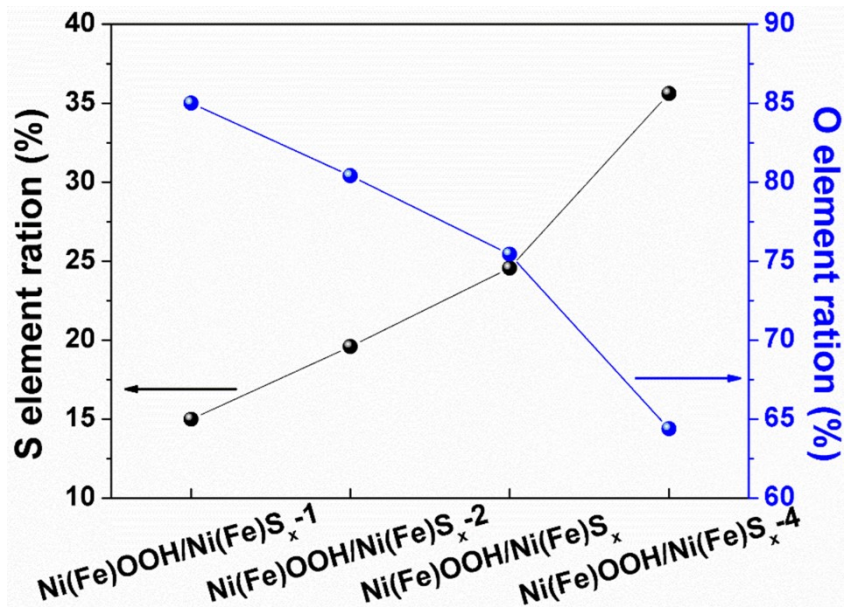Figure s15 (a), (b) SEM images of the Ni(Fe)OOH/Ni(Fe)S$_x$-4; (c) EDS analysis of Ni(Fe)OOH/Ni(Fe)S$_x$-4 and corresponding element ratios.

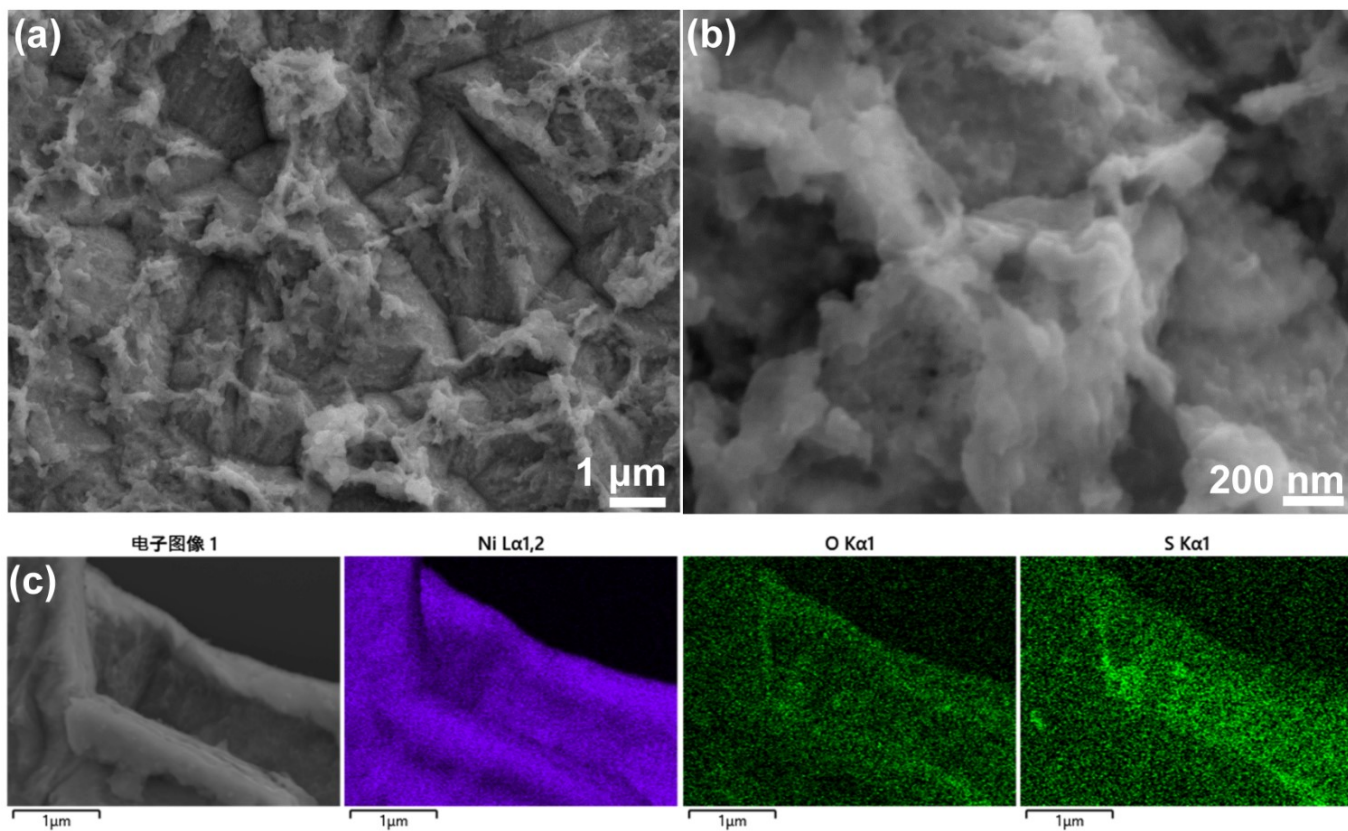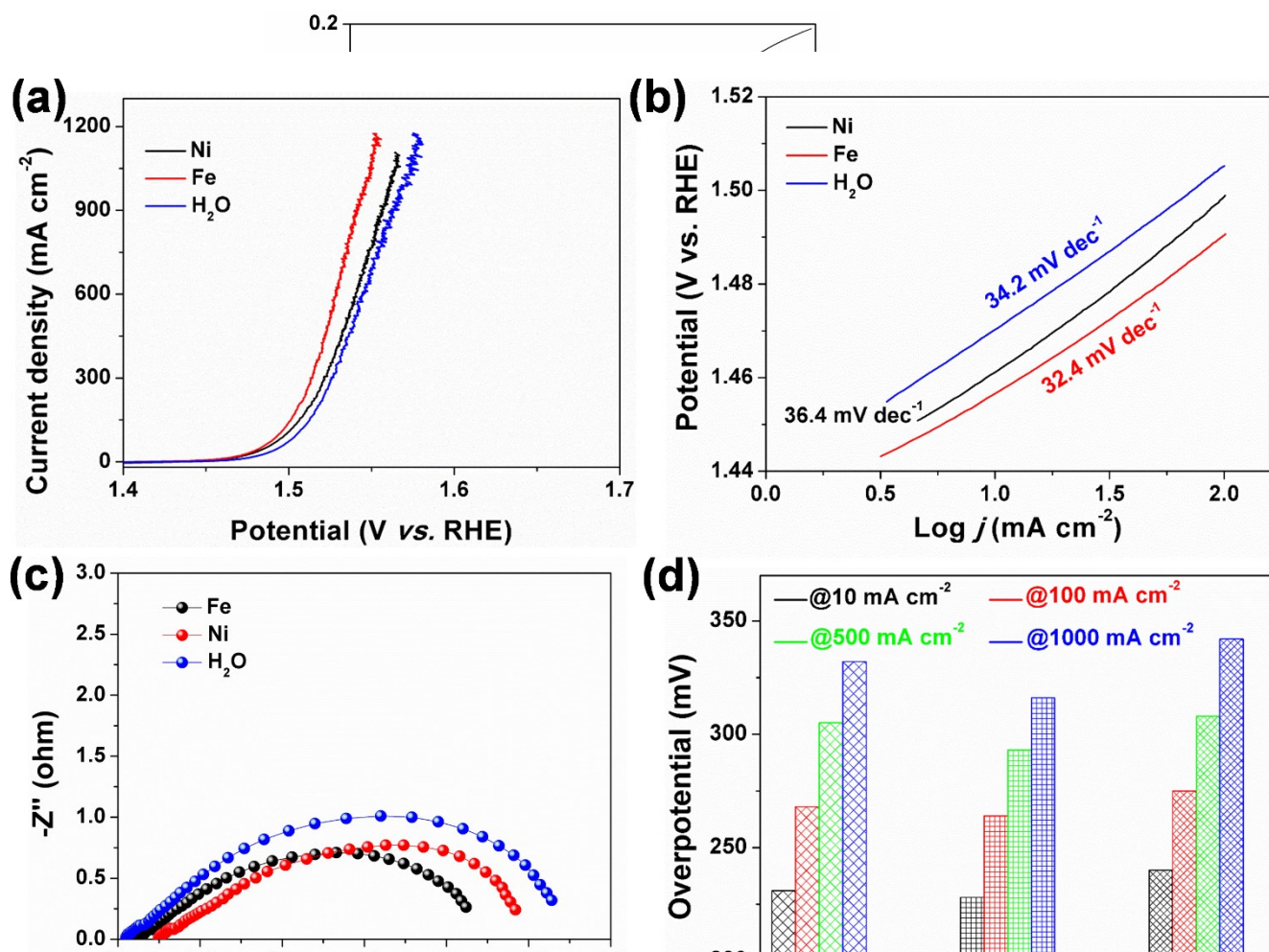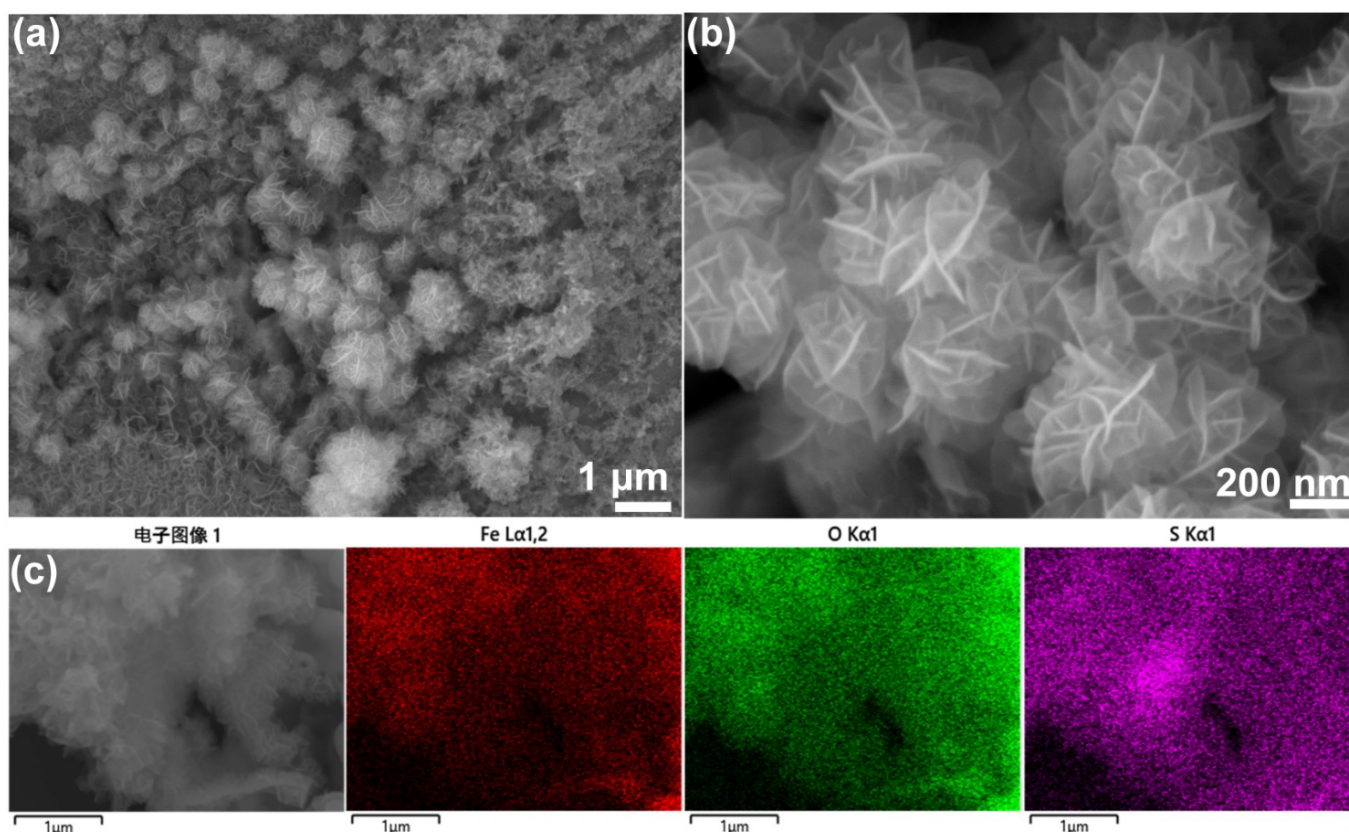Figure s16 the content of O and S elements in the samples

(a) ... 1 μm

(b) ... 200 nm

(c) 电子图像 1 | Ni Lα1,2 | O Kα1 | S Kα1

Figure s17 (a), (b) SEM images of the NiOOH/NiS$_x$ and (c) corresponding elemental mapping images.

Figure s18 (a), (b) SEM images of the FeOOH/FeS$_x$ and (c) corresponding elemental mapping images.

Figure s20 (a) OER polarization curves with iR-compensation and (b) corresponding Tafel slopes of various samples; (c) electrochemical impedance spectroscopy; (d) Overpotantials at 10, 100, 500, and 1000 mA cm^{-2}.
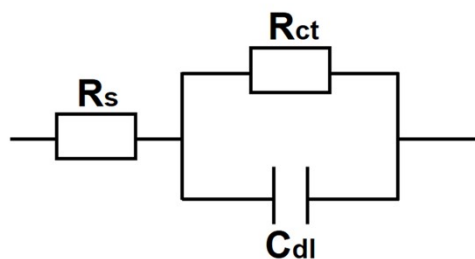
Figure s21 Equivalent circuit for the EIS Nyquist plots. (Rs: series resistance; Rct: charge transfer resistance; and C_{dl}: interface capacitance.)
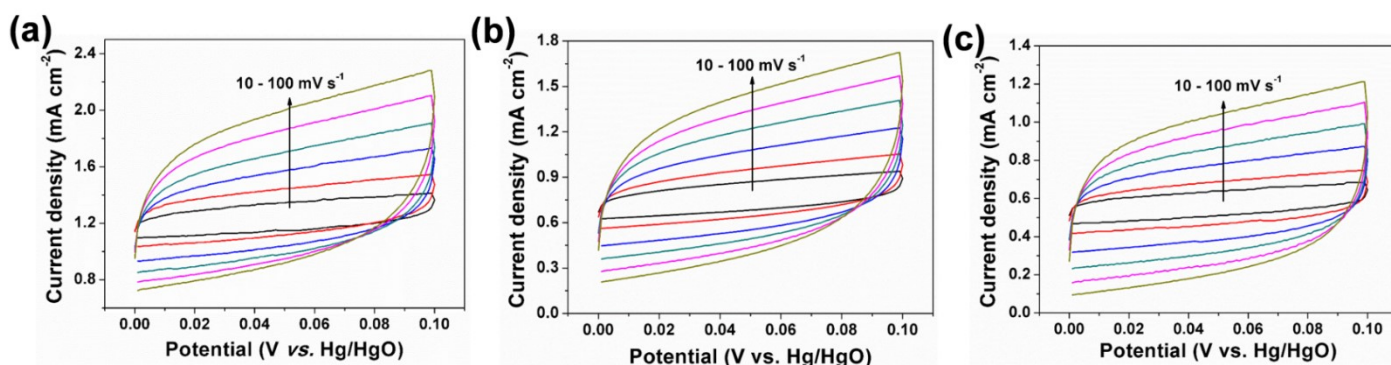

Figure s22 Cyclic voltammetry curves measured at different scan rates for (a) Ni(Fe)OOH/Ni(Fe)S_x-Ni, (b) Ni(Fe)OOH/Ni(Fe)S_x, and (c) Ni(Fe)OOH/Ni(Fe)S_x-H_2O.
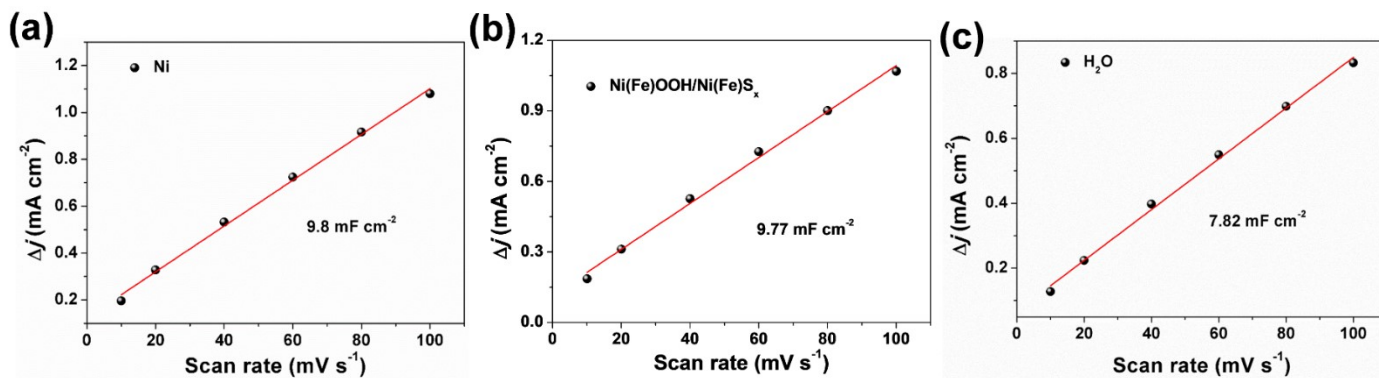

Figure s23 Electrochemical double-layer capacitances for (a) Ni(Fe)OOH/Ni(Fe)S_x-Ni, (b) Ni(Fe)OOH/Ni(Fe)S_x, and (c) Ni(Fe)OOH/Ni(Fe)S_x-H_2O.
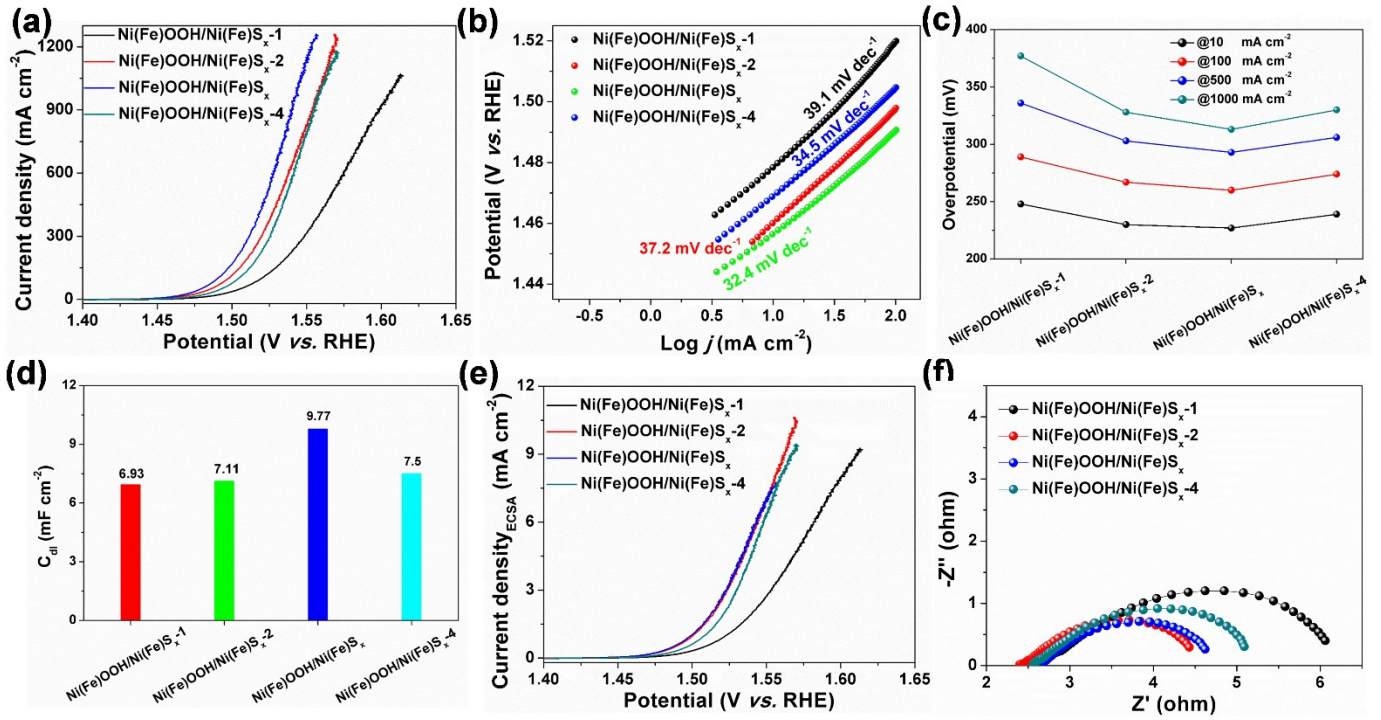
Figure s24 (a) OER polarization curves with iR-compensation and (b) corresponding Tafel slopes of various samples; (c) Overpotantials at 10, 100, 500, and 1000 mA cm^{-2}; (d) double-layer capacitances; (e) normalized OER polarization curves; (f) electrochemical impedance spectroscopy.
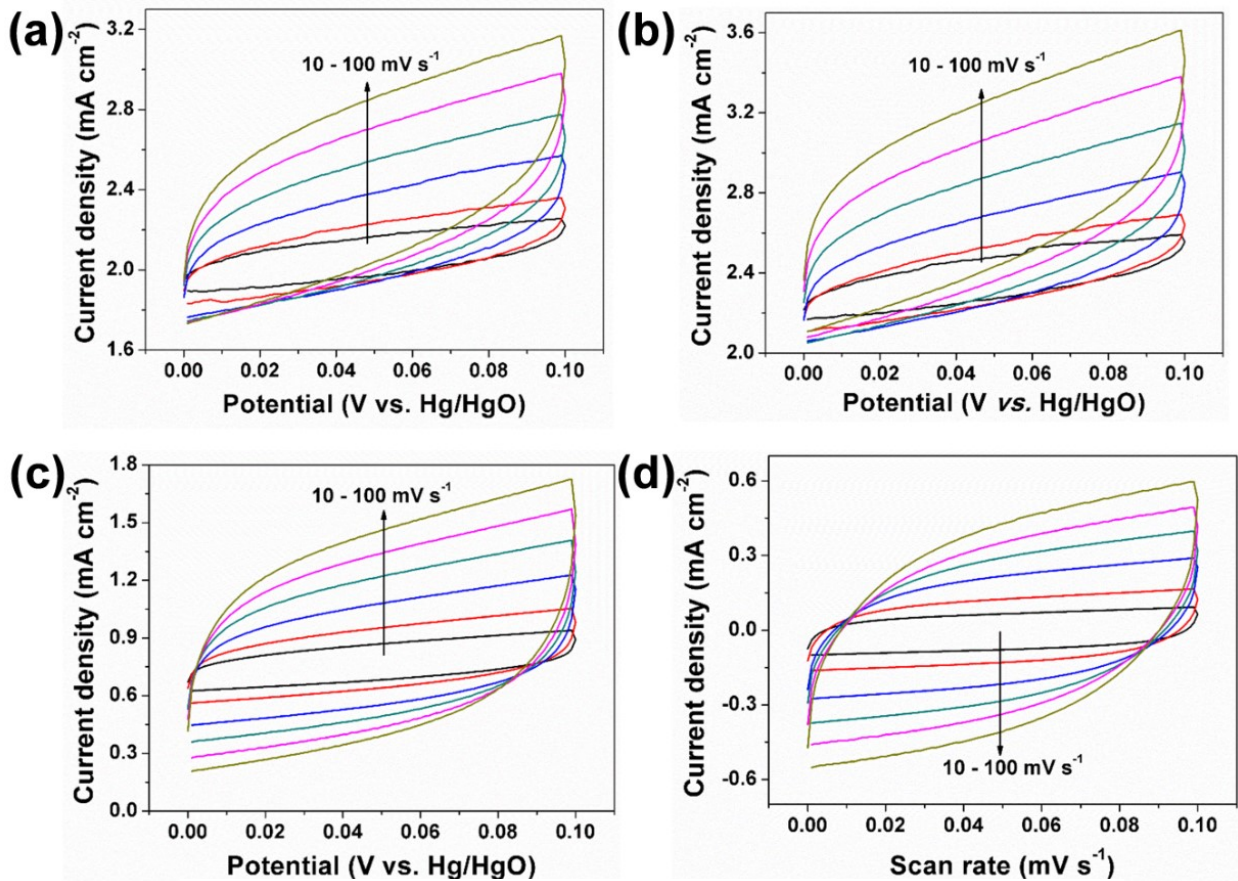
Figure s25 Cyclic voltammetry curves measured at different scan rates for (a) Ni(Fe)OOH/Ni(Fe)S$_x$-1, (b) Ni(Fe)OOH/Ni(Fe)S$_x$-2, (c) Ni(Fe)OOH/Ni(Fe)S$_x$, and (d) Ni(Fe)OOH/Ni(Fe)S$_x$-4.
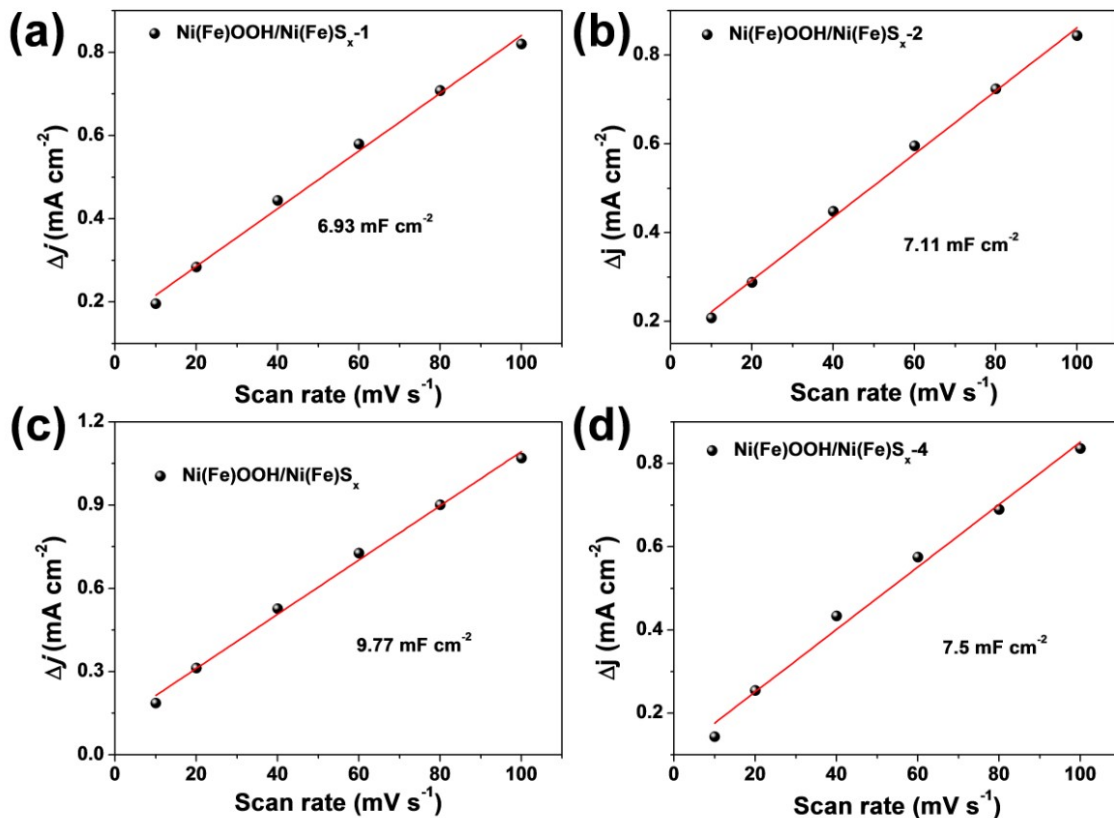

Figure s26 Electrochemical double-layer capacitances for (a) Ni(Fe)OOH/Ni(Fe)S$_x$-1, (b) Ni(Fe)OOH/Ni(Fe)S$_x$-2, (c) Ni(Fe)OOH/Ni(Fe)S$_x$, and (d) Ni(Fe)OOH/Ni(Fe)S$_x$-4.
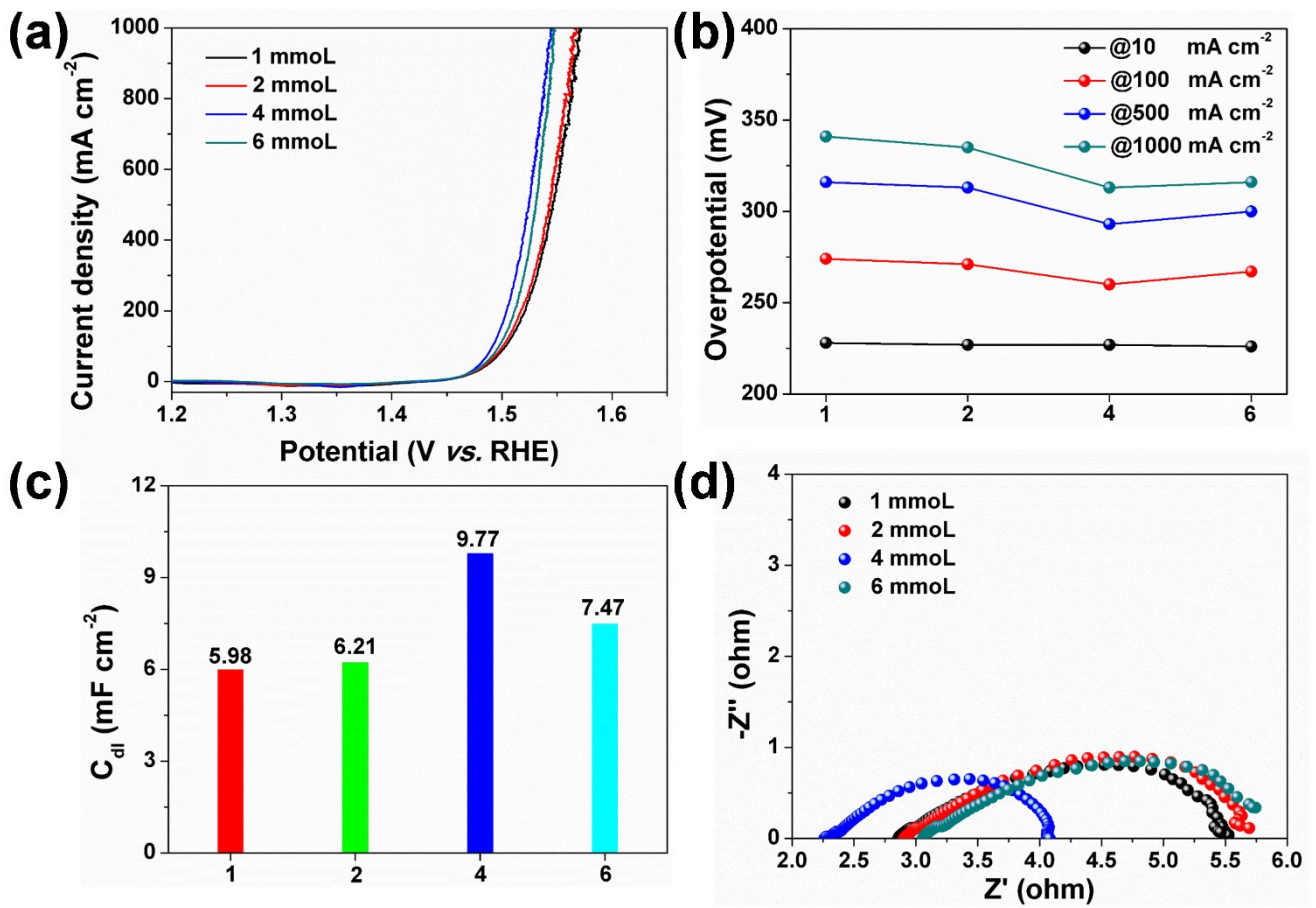
Figure s27 (a) OER polarization curves with iR-compensation and (b) Overpotentials at 10, 100, 500, and 1000 mA cm^{-2}. (c) double-layer capacitances; (d) electrochemical impedance spectroscopy.
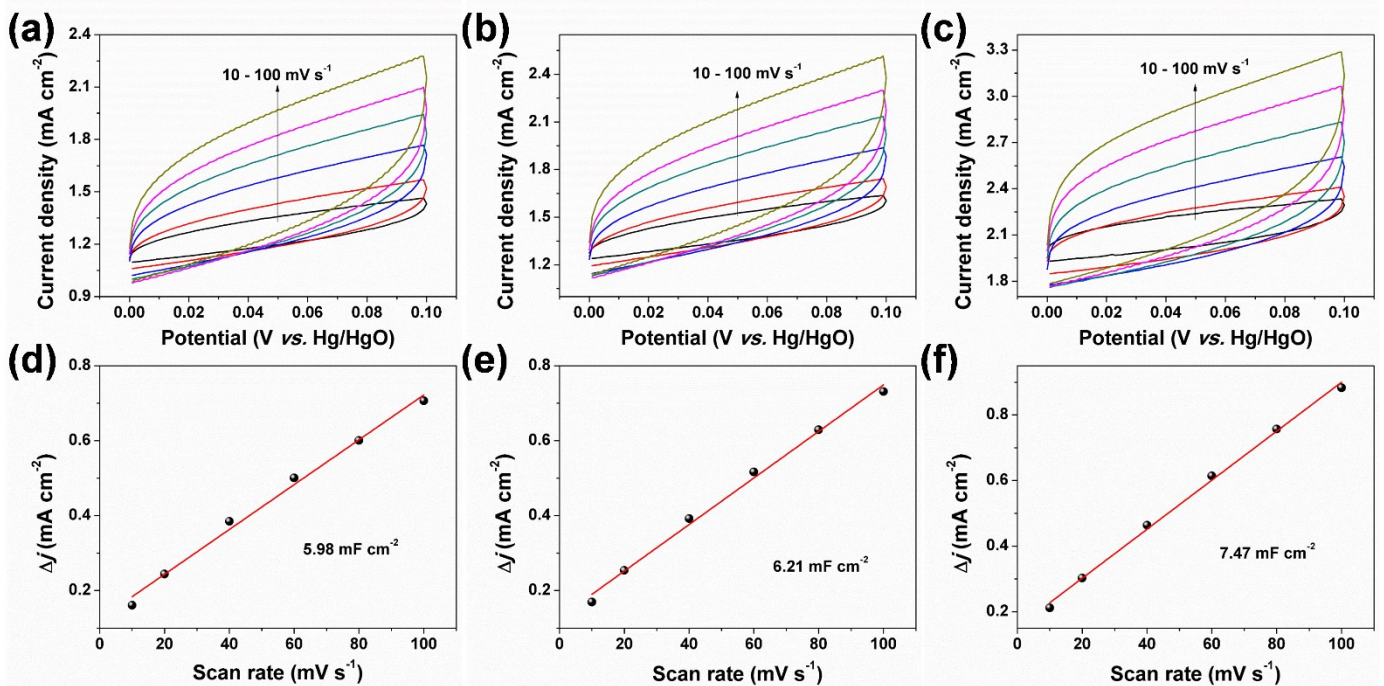

Figure s28 Cyclic voltammetry curves measured at different scan rates for (a) Ni(Fe)OOH/Ni(Fe)S$_x$-01, (b) Ni(Fe)OOH/Ni(Fe)S$_x$-02, and (c) Ni(Fe)OOH/Ni(Fe)S$_x$-06.
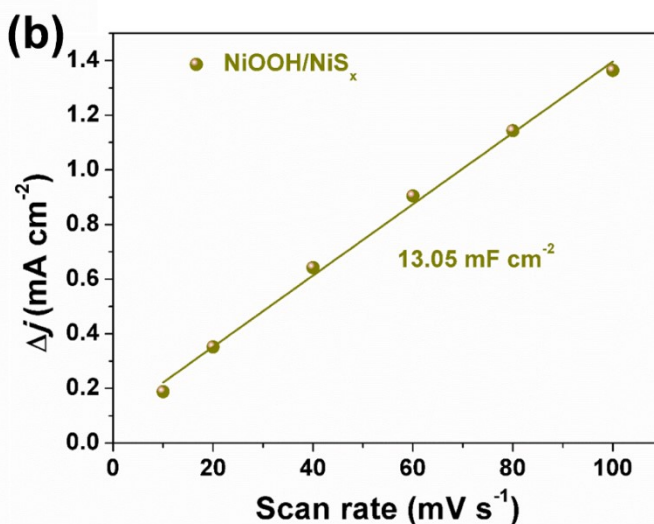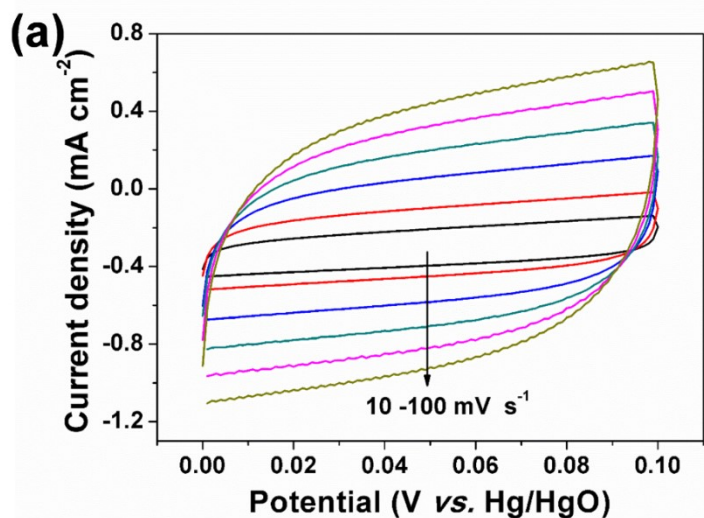
Figure s29 Cyclic voltammetry curves measured at different scan rates (a) and corresponding electrochemical double-layer capacitances (b) for $NiOOH/NiS_x$.

Figure s30 Cyclic voltammetry curves measured at different scan rates (a) and corresponding electrochemical double-layer capacitances (b) for $FeOOH/FeS_x$.
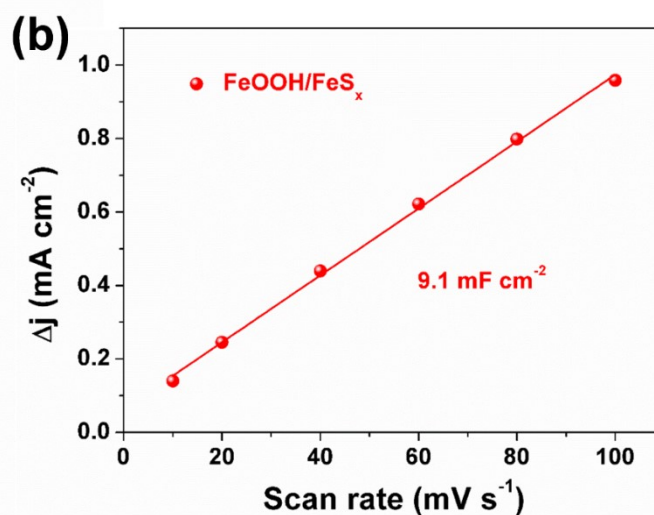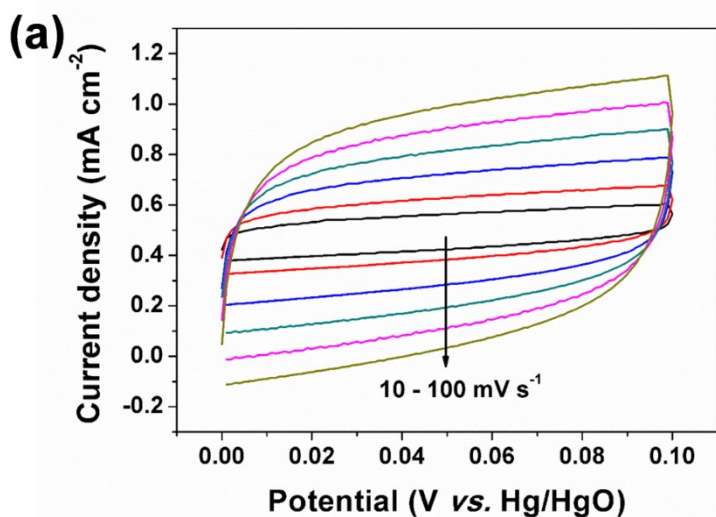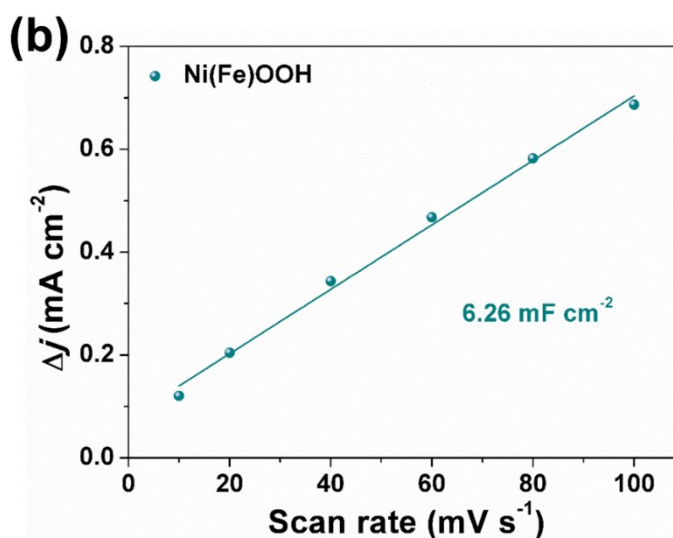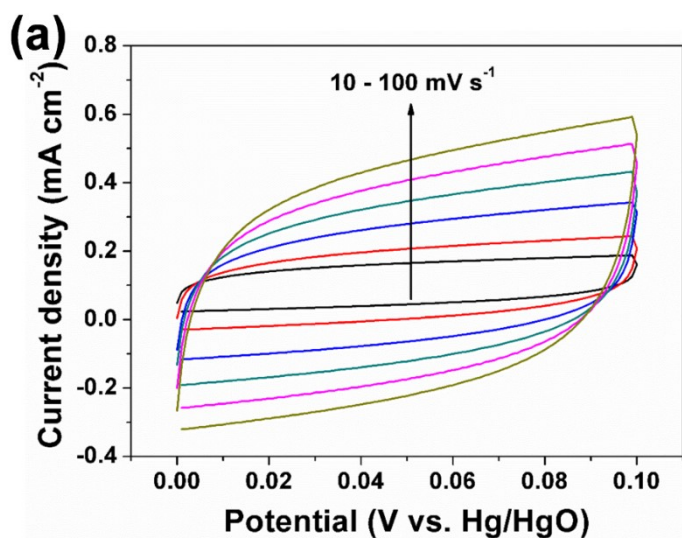

Figure s31 Cyclic voltammetry curves measured at different scan rates (a) and corresponding electrochemical double-layer capacitances (b) for Ni(Fe)OOH.
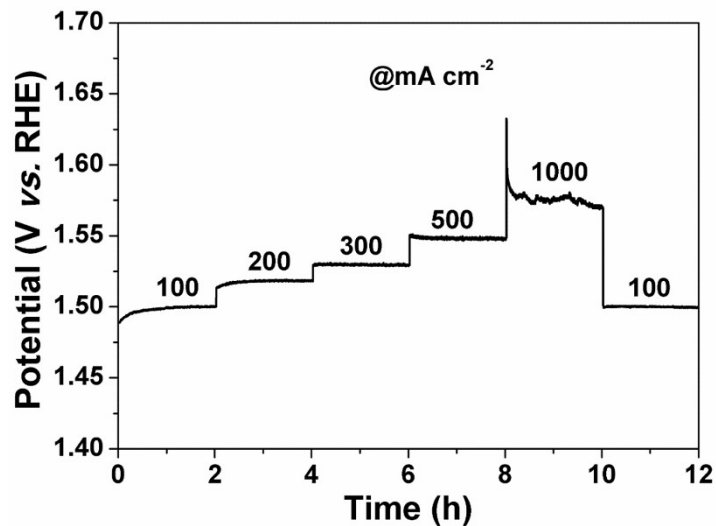
Figure 32 Multistep chronopotentiometric test at various current densities.

0 min   20 min   40 min   60 min   80 min   100 min
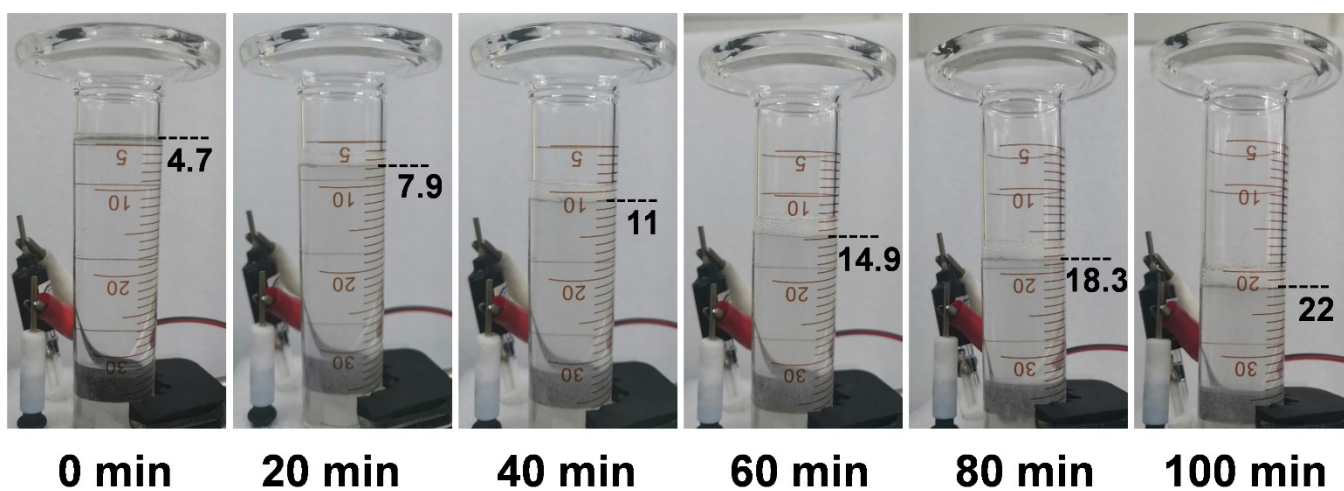
Figure 33 Photograph of the home-made setup for measuring O_2 generated from the Ni(Fe)OOH/Ni(Fe)S$_x$ electrode at a current density of 50 mA cm^{-2}.
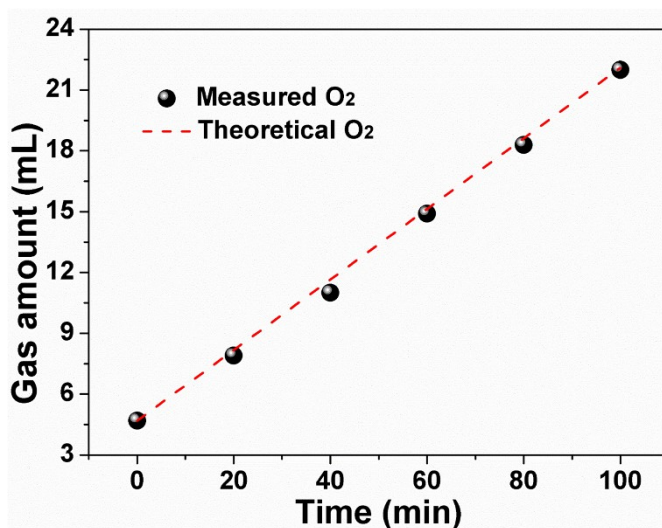
Figure 34 Experimental and theoretical amounts of O2 by the Ni(Fe)OOH/Ni(Fe)S$_x$ electrode at a current density of 50 mA cm^{-2}.
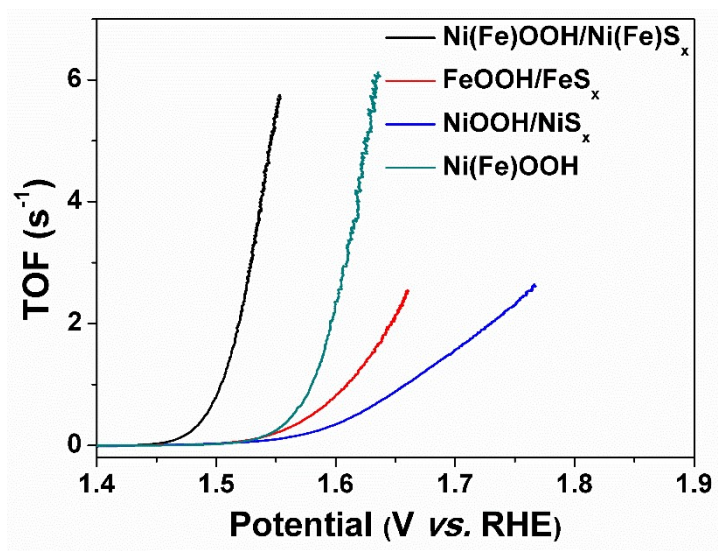
Figure 35 TOF curves of various samples.
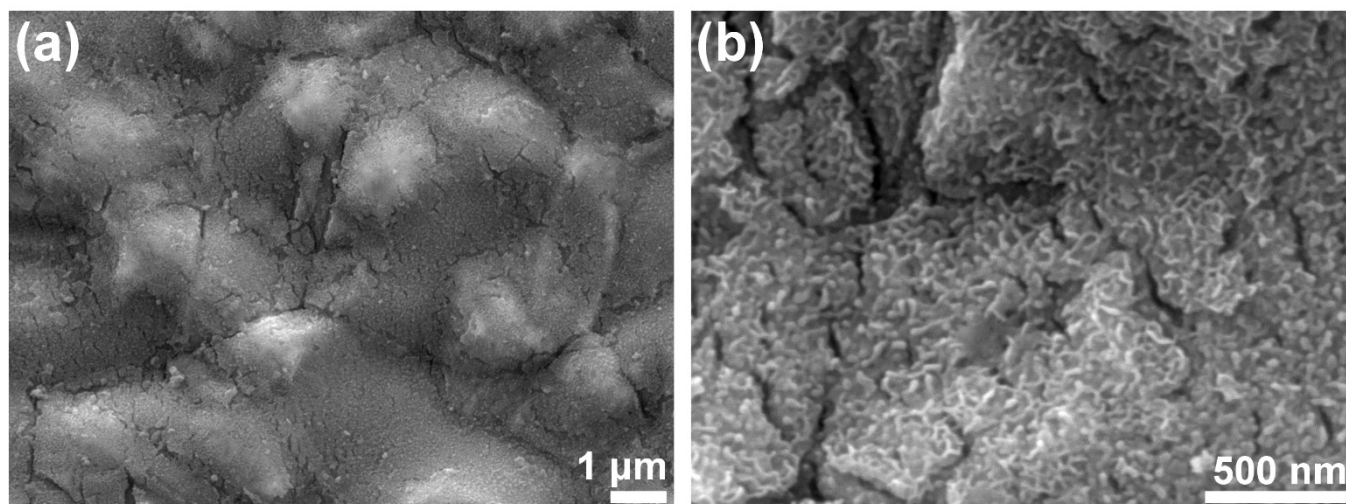
Figure 36 SEM images of Ni(Fe)OOH/Ni(Fe)S$_x$ after OER stability testing in 1 M KOH aqueous solution.
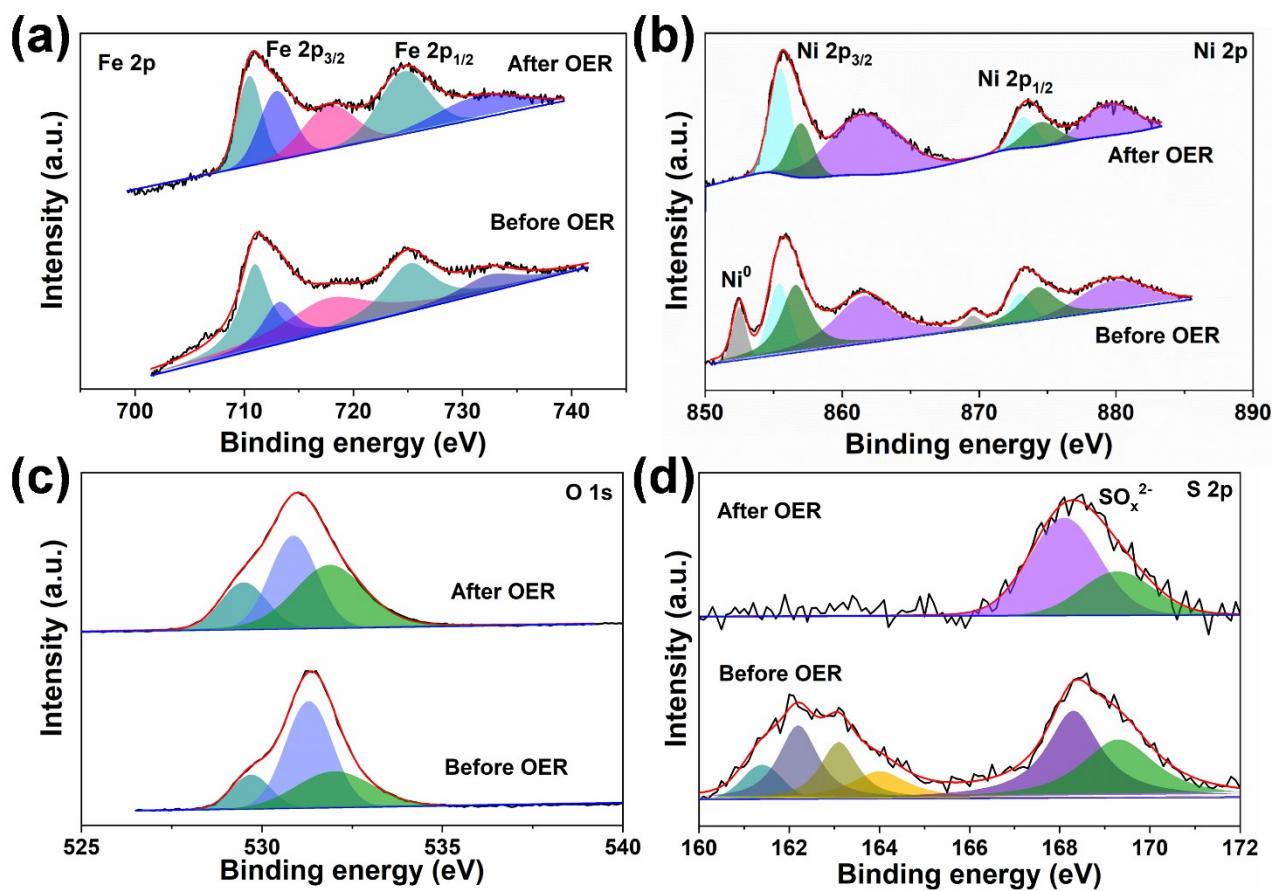
Figure 37 High-resolution XPS spectra of (a) Fe 2p, (b) Ni 2p, (c) O 1s, and (d) S 2p for Ni(Fe)OOH/Ni(Fe)S$_x$ before and after OER stability testing in 1 M KOH aqueous solution.
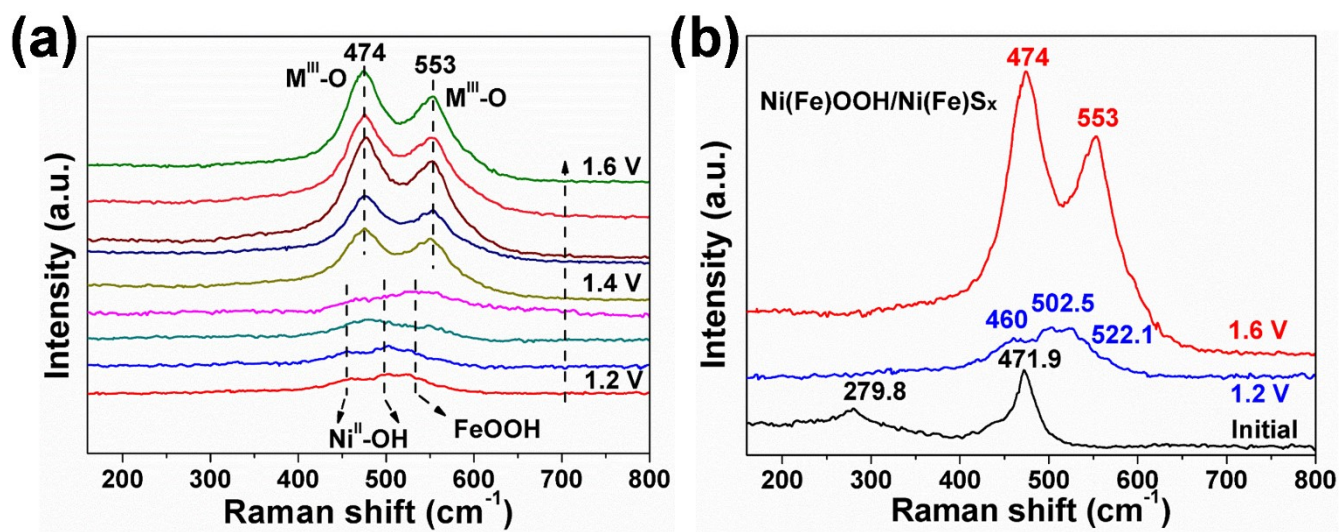
Figure 38 (a) *In situ* Raman spectra collected from Ni(Fe)OOH/Ni(Fe)S_x during OER process in 1 M KOH at various potentials vs. RHE; (b) Raman spectra collected under initial and specific potentials vs. RHE.
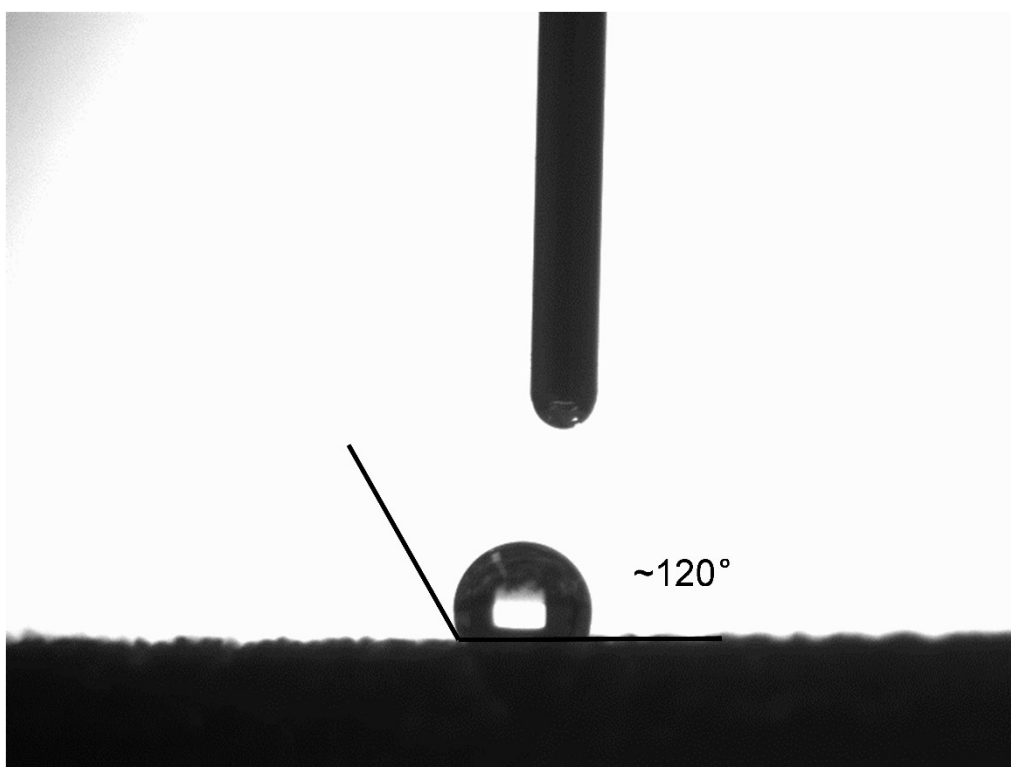
Figure s39 Contact angle measurement of NiFe foam.
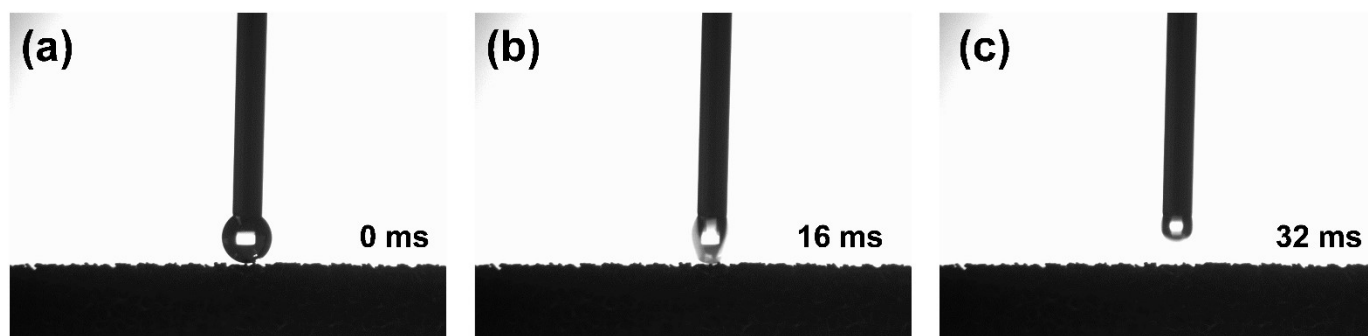
Figure s40 Contact angle measurement of Ni(Fe)OOH/Ni(Fe)S_x nanosheets array, and the contact angles of the Ni(Fe)OOH/Ni(Fe)S_x is about 0°.
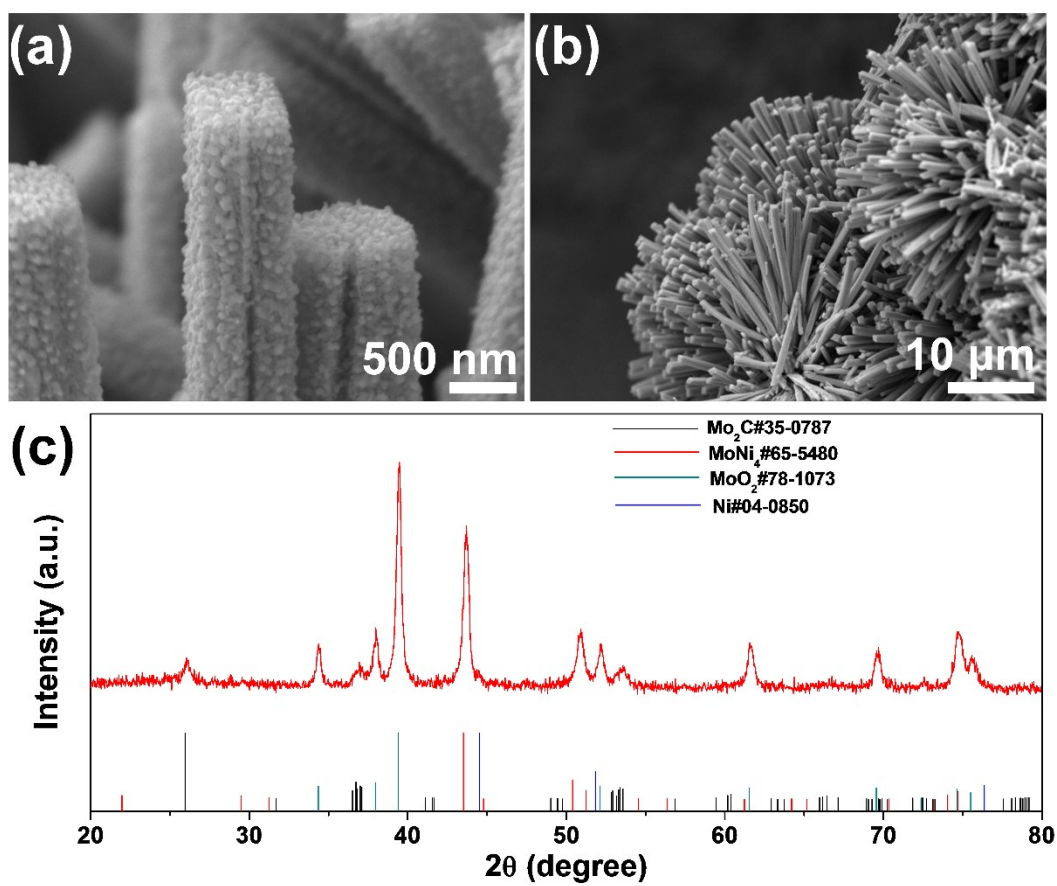
Figure s41 (a), (b) SEM images and (c) XRD pattern of the $Mo_2C/MoO_2/MoNi_4$.
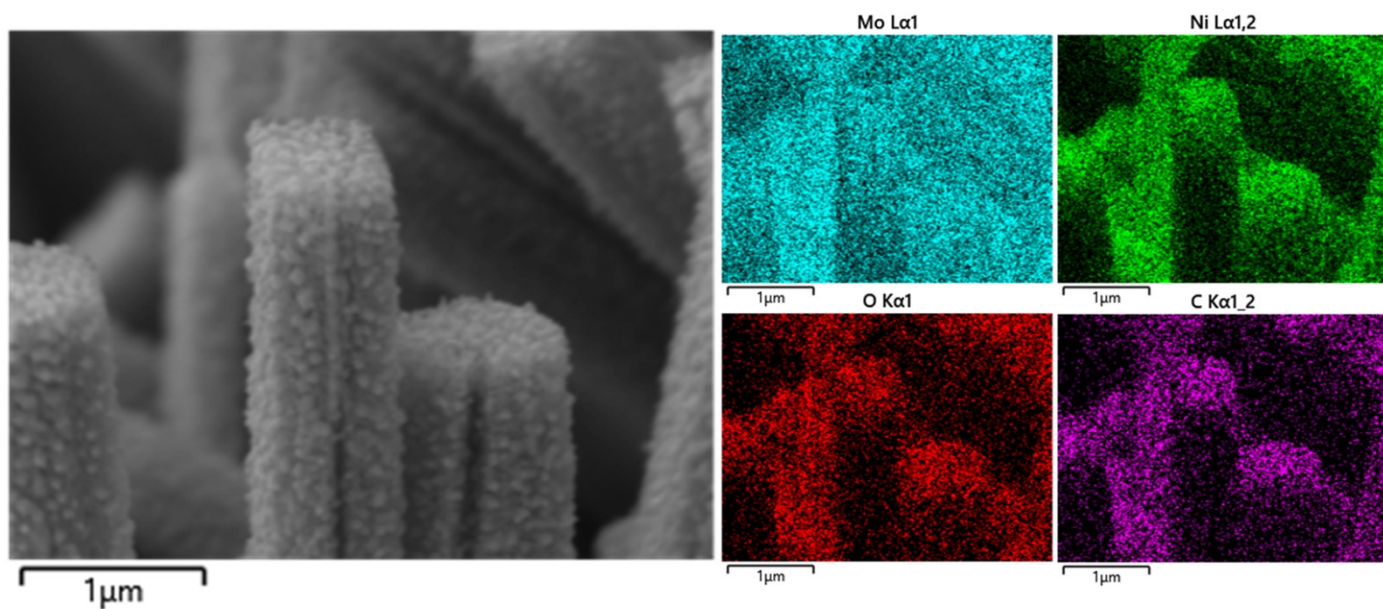
Figure s42 Elemental mapping images of $Mo_2C/MoO_2/MoNi_4$.
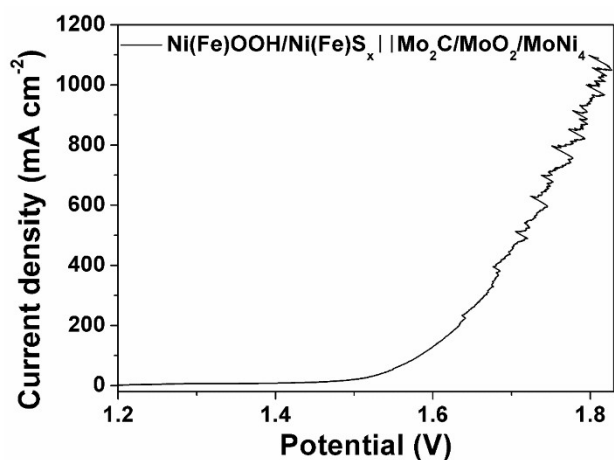
Current density (mA cm^{-2})	Potential (V)
η = 10	1.438
η = 100	1.583
η = 500	1.707
η = 1000	1.809

Figure s43 Polarzation curves using Ni(Fe)OOH/Ni(Fe)S$_x$ and Mo$_2$C/MoO$_2$/MoNi$_4$ as the cathode and anode, respectively, and corresponding the required potential at current density of 10, 100, 500, and 1000 mA cm^{-2} in 1M KOH aqueous solution at room temperature.

Table s1. Comparison of OER performances in 1 M KOH solution for Ni(Fe)OOH/Ni(Fe)S$_x$ with other electrodes.

OER catalyst	$\eta10$ (mV)	Tafel slope (mV dec^{-1})	Reference
Ni(Fe)OOH/Ni(Fe)S$_x$	227	32.4	This work
FeOOH/Ni$_3$N	244	67	*Applied Catalysis B: Environmental 269 (2020) 118600*
Co-Cu@GDY	234	51.7	*Nano Energy 74 (2020) 104852*
FeNi$_2$S$_4$	250	62	*Nano Energy 81 (2021) 105619*
L-Co$_3$O$_4$ NSs	290	76	*Nano Energy 83 (2021) 105800*
O-CoP-2	310	83.5	*Adv. Funct. Mater.* **2019**, 1905252
Co/TaS$_2$-3	330	70	*ACS Nano 2021, 15, 7105–7113*
Co$_x$(V$_{1-x}$)	282	56	*Adv. Energy Mater.* **2019**, 1903571

Co$_{0.85}$Se$_{1-x}$@C	231	57	*Adv. Mater.* **2021**, 2007523
CoP-InNC@CNT	270	84	*Adv. Sci.* **2020**, *7*, 1903195
NiFe-MOF/G	258	49	*Adv. Energy Mater*. **2021**, 2003759
MOF-FeCo(1:2)	238	52	Angew.Chem.2021,133,12204–12209
Fe$_{0.4}$Co$_{0.6}$Se$_2$	270	36	*Energy Environ. Sci.*, 2021, 14, 365--373
30%Ce-Ni-Fe-LDH	242	34	*Energy Environ. Sci.*, 2020, 13, 2949--2956
EO Co$_3$Mo/Cu	261	82	*Nat Commun* **11,** 2940 (2020)
FeNiCoCrMn-G	229	40	*Adv. Sci.* **2021**, 2002446
EA-Cu@Fe@Ni	240	47	*Nano Energy 81 (2021) 105644*
CoSAs-MoS$_2$/TiN NRs	340.6	73.5	*Adv. Funct. Mater.* **2021**, 2100233
IrCo@NC-850	302	52	*Adv. Funct. Mater.* **2021**, 2101797
Ag@Co(OH)x/CC	250	76	Angew. Chem. Int. Ed. **2020**, 59, 7245-7250
CoS/MoS$_2$	281	79	*Chem. Commun.*, **2021**, 57, 4847-4850
Ni$_3$FeN	259	54	Nano-Micro Lett. (2020) 12:79
NiCo$_2$S$_4$ NW/NF	260	40.1	*Adv. Funct. Mater.* **2016**, *26*, 4661－4672
r-FeOOH/NF-6M	286	51	*Adv. Mater.* **2021**, 2005587
Co$_5$Fe$_3$Cr$_2$	232	31	*Adv. Energy Mater*. **2021**, 2003412
FeOOH(Se)/IF	287	54	J. Am. Chem. Soc. 2019, 141, 7005−7013
Ni-CoP-5%	290	66	Nano Lett. 2021, 21, 823–832
NiFe LDH/NF-IH	246	46.6	*Adv. Funct. Mater.* **2021**, 2009580
NiFeV-LDH	287	53.7	*Adv. Funct. Mater.* **2021**, 2009743
Fe-x-Co$_9$S$_8$	255	49	*Adv. Energy Mater.* **2021**, *11*, 2003023
NiCo$_2$S$_4$@NiFe LDH	287	86.4	*Applied Catalysis B: Environmental 286 (2021) 119869*

Table s2. Comparision of OER stability of representative electrocatalysts in 1 M KOH solution.

Electrocatalyst	Current density	Time	Reference
Ni(Fe)OOH/Ni(Fe)S$_x$	100 mA cm^{-2}	100 h	This work
H$_2$PO^{2-}/FeNi-LDH-V$_2$C	10 mA cm^{-2}	30000 s	*Applied Catalysis B: Environmental 297 (2021) 120474*
NiFe-PBA-gel-cal	50 mA cm^{-2}	50 h	*Adv. Sci.* **2022**, 2200146
EE-NiFe-LDH	100 mA cm^{-2}	24 h	*Applied Catalysis B: Environmental 298 (2021) 120580*
NiFeCoMnAl	10 mA cm^{-2}	50 h	*Applied Catalysis B: Environmental 301 (2022) 120764*
RuFeO$_x$	10 mA cm^{-2}	10 h	*Adv. Funct. Mater.* **2021**, *31*, 2101405
La(CrMnFeCo$_2$Ni)O$_3$	10 mA cm^{-2}	50 h	*Adv. Funct. Mater.* **2021**, *31*, 2101632
PDANF	23 mA cm^{-2}	100 h	*Applied Catalysis B: Environmental 302 (2022) 120833*
a-LNFBPO	10 mA cm^{-2}	300 h	*Adv. Energy Mater.* **2021**, *11*, 2100624
NiFe-MOF/G	10 mA cm^{-2}	32 h	*Adv. Energy Mater.* **2021**, *11*, 2003759
CeO$_2$/CoS$_{1.97}$	10 mA cm^{-2}	50 h	*Adv. Mater.* **2021**, *33*, 2102593
Co$_{0.85}$Se$_{1-x}$@C	20 mA cm^{-2}	50 h	*Adv. Mater.* **2021**, *33*, 2007523
FeNiCoCrMn-G	100 mA cm^{-2}	36 h	*Adv. Sci.* **2021**, *8*, 2002446

Table s3. Comparision of OWS performance in 1 M KOH for the Ni(Fe)OOH/Ni(Fe)S_x||Mo_2C/MoO_2/$MoNi_4$ with other electrodes.

OWS catalyst	Cell voltage (η10)	Cell voltage (η100)	Reference
Ni(Fe)OOH/Ni(Fe)S_x||Mo_2C/MoO_2/$MoNi_4$	1.42 V	1.58 V	This work
Ru1/D-NiFe LDH	1.44	1.54	*Nat Commun* **12,** 4587 (2021)
NiFeRh-LDH	1.455	1.565	*Applied Catalysis B: Environmental 284 (2021) 119740*
Co-Fe-P	1.46	—	*Chemical Engineering Journal 405 (2021) 127002*
IrNi-FeNi$_3$	1.47	—	*Applied Catalysis B: Environmental 286 (2021) 119881*
Co$_3$O$_4$-Ag	1.49	—	*Applied Catalysis B: Environmental 299 (2021) 120658*
MoS$_2$-Mo$_2$C	1.49	—	*Nano Energy 88 (2021) 106277*
Ni$_3$Se$_2$@NiOOH	1.52	—	*Sci China Mater 2019, 62(8): 1096–1104*
NiCo(-)//NiFe(+)	1.52	1.64	*Applied Catalysis B: Environmental 288 (2021) 120002*
NiMnFeMo	1.54	—	*Chemical Engineering Journal 404 (2021) 126530*
CoMoN$_x$-500	1.55	—	*Chemical Engineering Journal 411 (2021) 128433*
Fe-Ni$_5$P$_4$/NiFeOH	1.55	—	*Applied Catalysis B: Environmental 291 (2021) 119987*
NiP$_2$/NiSe$_2$	1.56	1.8	*Applied Catalysis B: Environmental 282 (2021) 119584*
E-NiFeOOH	1.59	—	J. Mater. Chem. A, 2021, 9, 20058
Ni$_3$S$_2$/FeS	1.61	—	*Journal of Power Sources 487 (2021) 229408*
Te/Fe-NiOOH	1.65	—	ACS Appl. Mater. Interfaces 2021, 13, 10972−10978
P@*p*CoPc-1/Co$_3$O$_4$|CC	1.672	—	*Adv. Funct. Mater.* **2021**, *31*, 2103290
CoP@FeCoP	1.68	—	*Chemical Engineering Journal 403 (2021) 126312*
CF/VMFO	1.37	1.59	*Nat Commun* **12,** 1380 (2021)

FeP/Ni$_2$P	—	1.6	*Nat Commun **9,** 2551 (2018)*
Ni$_2$P/Ni$_3$S$_2$	1.5	1.62	*Nano Energy 51 (2018) 26 – 36*
Ni$_{0.5}$Mo$_{0.5}$OSe	1.51	1.63	*Applied Catalysis B: Environmental 286 (2021) 119909*
NiFeP-MoO$_2$	1.41	1.65	*Chemical Engineering Journal 409 (2021) 128161*
Fe-FVO-60-act	1.58	1.72	*Chemical Engineering Journal 416 (2021) 129165*
NiCoP	1.59	1.73	Nanoscale, 2021, 13, 14179
CoS$_2$/MoS$_2$	1.59	1.74	*ChemSusChem 2021, 14, 699 – 708*
MoS$_2$/Fe$_5$Ni$_4$S$_8$	—	1.78	*Adv. Mater. **2018**, 30, 1803151*
Ni-ZIF/Ni-B@NF-4	1.54	1.78	*Adv. Energy Mater. **2020**, 10, 1902714*
Mo-Ni$_3$S$_2$/NixPy	1.46	1.8	*Adv. Energy Mater. **2020**, 10, 1903891*
Ni$_3$S$_2$/FeNi$_2$S$_4$	1.55	1.86	*Chemical Engineering Journal 427 (2022) 131944*
NiFe LDH@NiCoP/NF	1.57	1.9	*Adv. Funct. Mater. **2018**, 28, 1706847*
NiCo$_2$S$_4$	1.58	1.94	*Adv. Funct. Mater. **2019**, 29, 1807031*

Table s4. Comparision of OWS stability of representative electrocatalysts in 1 M KOH solution.

OWS catalyst	Current density	Time	Reference
Ni(Fe)OOH/Ni(Fe)S$_x$‖ Mo$_2$C/MoO$_2$/MoNi$_4$	100 mA cm^{-2}	100 h	This work
CoP@CoOOH	10 mA cm^{-2}	140 h	*Small* **2022**, *18*, 2106012
Ni/CeO$_2$@N-CNFs	10 mA cm^{-2}	100 h	*Small* **2022**, *18*, 2106592
NCRO-4	10 mA cm^{-2}	200 h	*Applied Catalysis B: Environmental 305 (2022) 121081*
Pt/C‖vs-Ru-Ni$_9$S$_8$	10 mA cm^{-2}	100 h	*Applied Catalysis B: Environmental 310 (2022) 121356*
Ni$_2$P—CuP$_2$	10 mA cm^{-2}	40 h	ACS Nano 2021, 15, 5586−5599
LIA-Ni-BDC‖LIA-MIL-101(Fe)	50 mA cm^{-2}	50 h	*Adv. Funct. Mater.* **2021**, *31*, 2102648
Pd/NiFeO$_x$	20 mA cm^{-2}	50 h	*Adv. Funct. Mater.* **2021**, *31*, 2107181
CoNiRu-NT	50 mA cm^{-2}	48 h	*Adv. Mater.* **2022**, *34*, 2107488
NiFe-PBA-gel-cal	100 mA cm^{-2}	50 h	*Adv. Sci.* **2022**, 2200146
IrO$_2$/V$_2$O$_5$	10 mA cm^{-2}	30 h	*Adv. Sci.* **2022**, 2104636